UNDER FREQUENCY LOAD SHEDDING SCHEME FOR ISLANDED DISTRIBUTION SYSTEM BASED ON MIXED INTEGER LINEAR PROGRAMMING

SOHAIL SARWAR

FACULTY OF ENGINEERING
UNIVERSITY OF MALAYA
KUALA LUMPUR

2020

UNDER FREQUENCY LOAD SHEDDING SCHEME FOR ISLANDED DISTRIBUTION SYSTEM BASED ON MIXED INTEGER LINEAR PROGRAMMING

SOHAIL SARWAR

DISSERTATION SUBMITTED IN FULFILMENT OF THE REQUIREMENTS FOR THE DEGREE OF MASTER'S IN ENGINEERING SCIENCES

FACULTY OF ENGINEERING
UNIVERSITY OF MALAYA
KUALA LUMPUR

2020

UNIVERSITY OF MALAYA

ORIGINAL LITERARY WORK DECLARATION

Name of Candidate: Sohail Sarwar

Matric No: KGA180013

Name of Degree: Master's in engineering sciences

Title of Dissertation ("this Work"):

UNDER FREQUENCY LOAD SHEDDING SCHEME FOR ISLANDED DISTRIBUTION SYSTEM BASED ON MIXED INTEGER LINEAR PROGRAMMING.

Field of Study: Electrical Engineering (Power Systems)

I do solemnly and sincerely declare that:

(1) I am the sole author/writer of this Work;

(2) This Work is original;

(3) Any use of any work in which copyright exists was done by way of fair dealing and for permitted purposes and any excerpt or extract from, or reference to or reproduction of any copyright work has been disclosed expressly and sufficiently and the title of the Work and its authorship have been acknowledged in this Work;

(4) I do not have any actual knowledge nor do I ought reasonably to know that the making of this work constitutes an infringement of any copyright work;

(5) I hereby assign all and every rights in the copyright to this Work to the University of Malaya ("UM"), who henceforth shall be owner of the copyright in this Work and that any reproduction or use in any form or by any means whatsoever is prohibited without the written consent of UM having been first had and obtained;

(6) I am fully aware that if in the course of making this Work I have infringed any copyright whether intentionally or otherwise, I may be subject to legal action or any other action as may be determined by UM.

Candidate's Signature Date:

Subscribed and solemnly declared before,

Witness's Signature Date:

Name:

Designation:

UNDER FREQUENCY LOAD SHEDDING SCHEME FOR ISLANDED DISTRIBUTION SYSTEM BASED ON MIXED INTEGER LINEAR PROGRAMMING.

ABSTRACT

In recent years, significant climate changes have pivoted the distribution system towards utilization of renewable energy, particularly through distributed generators (DGs). Although DGs offer many benefits, its integration affects the stability of the system, which could lead to blackout, when the grid is disconnected. The system frequency will drop drastically if DG's generation capacity is less than the total load demand in the network. In order to sustain the system stability, Under Frequency Load Shedding (UFLS) is a commonly used technique to minimize the difference in load demand and power generation. However, existing load shedding techniques are lack in accurate estimation of power imbalance. Conventional load shedding sheds random loads sequentially until the system's frequency is recovered. Random and sequential selection of loads without priority results in excessive load shedding, which in turn causes frequency overshoot. Thus, a technique yielding an optimal solution for load shedding incorporating load priority is needed. In this regard, this work proposes an efficient load shedding technique for islanded distribution system. This technique utilizes voltage stability index to rank the unstable loads for load shedding. In the proposed technique, polynomial regression is used to establish a function of power imbalance in the form of frequency decay. Mixed Integer Linear Programming (MILP) optimization produces optimal load shedding strategy based on the priority of the loads (i.e., non-critical, semi-critical, and critical) and the load ranking from voltage stability index. The effectiveness of the proposed technique is tested on three test systems, i.e., 28 bus system, which is a part of the Malaysian distribution network, the IEEE 69 bus system, and the IEEE 137 bus system, using PSCAD/EMTDC. Results obtained prove the effectiveness of the proposed technique in stabilizing the system's frequency without overshoot by disconnecting unstable non-critical loads on priority. Furthermore, results show that the proposed technique is superior compared to other adaptive techniques on the basis it increases sustainability by reducing the load shed amount and avoiding overshoot in system frequency. Also, its performance is not affected by increasing the number of loads for a large-scale system.

Keywords: Frequency instability; Cascaded Blackout; Under frequency load Shedding; Load priority; Polynomial regression; Mixed-integer linear programming

ABSTRAK

Beberapa tahun lepas, perubahan iklim yang signifikan mendorong sistem pengedaran ke arah tenaga boleh diperbaharui, terutama melalui generator yang diedarkan (DG). Walaupun, DG menawarkan banyak manfaat untuk sistem pengedaran, integrasinya mempengaruhi kestabilan sistem yang boleh menyebabkan bekalan elektrik terputus ketika jaringan terputus. Kekerapan sistem akan menurun secara drastik, jika kapasiti penjanaan DG kurang dari jumlah permintaan beban di rangkaian. Untuk menjaga kestabilan sistem, beban terbuang frekuensi rendah (UFLS) merupakan teknik yang selalu digunakan bagi meminimumkan perbezaan permintaan beban dan penjanaan tenaga. Walaubagaimanapun, teknik beban terbuang yang sedia ada tidak mampu memberikan anggaran yang tepat dari sudut ketidakseimbangan daya. Pendekatan umum beban terbuang menurunkan beban rawak secara berurutan sehingga frekuensi sistem pulih. Pemilihan beban secara rawak dan berurutan tanpa memberi keutamaan kepada beban terbuang yang berlebihan, yang seterusnya menyebabkan frekuensi berlebihan. Teknik yang menghasilkan penyelesaian yang optimum untuk pembebanan beban dengan memasukkan keutamaan beban yang diperlukan. Sehubungan dengan itu, tesis ini mencadangkan teknik pembebanan muatan yang efisien untuk sistem pengagihan pulau. Teknik ini menggunakan indeks kestabilan voltan untuk menentukan beban yang tidak stabil untuk beban terbuang. Dalam kaedah yang dicadangkan, regresi polinomial digunakan untuk menetapkan fungsi ketidakseimbangan kyasa dalam bentuk peluruhan frekuensi. Pengoptimuman pengaturcaraan linear integer campuran (MILP) menghasilkan strategi beban terbuang yang optimum berdasarkan keutamaan beban (iaitu, tidak kritikal, separa kritikal, dan kritikal) dan peringkat beban dari indeks kestabilan voltan. Keberkesanan teknik yang dicadangkan diuji pada tiga sistem ujian iaitu sistem bas 28, yang merupakan sebahagian daripada rangkaian pengedaran Malaysia, sistem bas IEEE 69 dan sistem bas IEEE 137, menggunakan PSCAD /

EMTDC. Keputusan yang diperoleh membuktikan keberkesanan teknik yang dicadangkan dalam menstabilkan frekuensi sistem tanpa berlibihan dengan memutuskan beban tidak kritikal yang tidak stabil pada keutamaan. Selanjutnya, hasil menunjukkan bahawa teknik yang diusulkan lebih unggul daripada teknik penyesuaian yang lain, kerana meningkatkan keberlanjutan dengan mengurangi jumlah beban terbuang dan menghindari lebihan frekuensi sistem. Juga, prestasinya tidak dipengaruhi oleh peningkatan jumlah beban untuk sistem berskala besar.

Kata kunci: Ketidakstabilan prekunsi; Pemadaman Lata; Di bawah frekuensi beban terbuang; Beban keutamaan; Regresi polinomial; Pengaturcaraan linear integer campuran

ACKNOWLEDGEMENTS

ALHAMDULILLAH, I would like to thank almighty Allah for giving me the mental health and physical strength to complete this journey of research.

Firstly, I would like to express my gratitude and heartiest appreciation to my supervisors, Professor Ir. Dr. Hazlie Bin Mokhlis and Dr. Mohamadariff Bin Othman for their guidance and support. Their devoted supervision and welcoming hands were always there for me in every situation.

I would also be thankful and grateful to my father Muhammad Sarwar, my dearest mother, my beloved wife and also my siblings for their endless love, prayers, support, and motivation, which enabled me to complete my studies.

Finally, I am grateful to higher education commission (HEC) of Pakistan and Govt. of Pakistan for financially supporting my study. I am also thankful to the University of Malaya for providing sufficient research facilities and supports.

TABLE OF CONTENTS

Abstract iii

Abstrak v

Acknowledgements vii

Table of Contents viii

List of Figures xii

List of Tables xiv

List of Abbreviations and Symbols xvi

CHAPTER 1: INTRODUCTION 1

1.1 Overview 1

1.2 Problem Statement 3

1.3 Research Objective 4

1.4 Research Methodology 5

1.5 Scope of Research 6

1.6 Dissertation Outline 7

CHAPTER 2: LITERATURE REVIEW 8

2.1 Introduction 8

2.2 Limitations of DGs 9

2.3 Under frequency load shedding 9

2.4 Conventional under frequency load shedding 10

2.5 Semi-Adaptive under frequency load shedding schemes 11

2.6 Intelligent under frequency load shedding 13

2.6.1 Intelligent LS schemes based on ANN... 14

2.6.2 Intelligent LS schemes based on Fuzzy logic 15

2.7 Adaptive under frequency load shedding 16

2.7.1 Adaptive LS schemes based on voltage stability index.......................... 19

2.7.2 Adaptive LS schemes based on optimal load selection.......................... 22

2.8 Summary 22

CHAPTER 3: PROPOSED UNDER FREQUENCY LOAD SHEDDING............. 25

3.1 Introduction... 25

3.2 Average System Frequency Calculation Module 26

3.3 Power imbalance forecasting module (PIFM).. 26

3.4 Stability Index Calculation Module (SICM) 29

3.5 Intelligent Load Shedding Module (ILSM).. 30

3.6 Test System modeling... 32

3.6.1 Malaysian 28 bus distribution system 32

3.6.2 IEEE 69 bus distribution System.. 36

3.6.3 IEEE 137 bus distribution System.. 40

3.6.4 Modeling of system equipment 40

3.6.5 Modeling of Conventional UFLS... 42

3.6.6 Modeling of UFLS Adaptive Techniques 43

3.7 Summary.. 44

CHAPTER 4: RESULTS AND DISCUSSIONS 46

4.1 Introduction.. 46

4.2 Development of power imbalance equation 46

4.3 Scenario I 49

4.3.1 Test results for 28 bus system (Scenario-I) 49

4.3.1.1 Islanding Event (Scenario-I) 50

4.3.1.2 DG tripping in islanded system (Scenario-I)............................. 53

4.3.1.3 Cascaded DG tripping in islanded system (Scenario-I) 55

4.4 Test results for IEEE 137 bus system 56

4.5 Scenario II... 59

4.5.1 Test results for the 28-bus system (Scenario-II)....................................... 59

4.5.1.1 Islanding Event (Scenario II) 60

4.5.1.2 DG Tripping in an Islanded System (Scenario II)..................... 63

4.5.1.3 Overloading event in islanded system (Scenario II) 66

4.5.2 Test results for IEEE 69 bus system... 69

4.5.2.1 Islanding Event (69-Bus System)... 69

4.5.2.2 DG-Tripping Event (IEEE 69-Bus System).............................. 72

4.6 Scenario III 74

4.6.1 Islanding Event (Scenario III) 75

4.6.2 DG Tripping in Islanded System (Scenario III) 77

4.7 Summary.. 79

CHAPTER 5: CONCLUSION AND FUTURE WORKS 80

5.1 Conclusion 80

5.2 Future works 81

References 83

List of Publications 88

LIST OF FIGURES

Figure 3.1: Block diagram of the proposed load shedding scheme. 25

Figure 3.2: Flow chart of the proposed PIFM module. 29

Figure 3.3: Flowchart of the proposed intelligent load shedding module (ILSM). 32

Figure 3.4: 11kV-28 bus Malaysian distribution system. 33

Figure 3.5: PSCAD modeling of 11kV-28 bus Malaysian distribution system. 34

Figure 3.6: IEEE 69 bus distribution system. 37

Figure 3.7: IEEE 137 bus system. 40

Figure 3.8: Synchronous generator model in PSCAD. 41

Figure 3.9: Comparison of SFR for multistep conventional load shedding. 43

Figure 4.1: Polynomial Regression for Power Imbalance. 47

Figure 4.2: Frequency Response for Different Polynomial PI Predictions. 48

Figure 4.3: Frequency Response for Islanding (Scenario-I). 52

Figure 4.4: Frequency Response for DG Tripping (Scenario-I). 54

Figure 4.5: Real-Time Total Load of the 28 Bus System (Scenario-I). 55

Figure 4.6: Frequency response for cascaded DG tripping. 56

Figure 4.7: Frequency response for IEEE 137 bus system. 57

Figure 4.8: System frequency response (SFR) for islanding event (Scenario II). 61

Figure 4.9: SFR for DG tripping event (Scenario II). 64

Figure 4.10: SFR for overloading event (Scenario II). 68

Figure 4.11: SFR comparison (IEEE 69-bus system). 70

Figure 4.12: SFR comparison for DG tripping event (IEEE 69-bus system). 73

Figure 4.13: SFR comparison for the proposed technique (Islanding). 76

Figure 4.14: SFR comparison for the proposed technique (DG tripping). 78

LIST OF TABLES

Table 2.1: Limitations of DG in grid-connected mode 9

Table 2.2: Limitations of distributed generation in islanded mode 9

Table 2.3: Comparison of semi-adaptive LS techniques 14

Table 2.4: Comparison of adaptive LS techniques 19

Table 3.1: Load data for 11kV-28 bus system. 35

Table 3.2: Optimal DG size and location (Muhammad et al., 2019). 36

Table 3.3: IEEE 69 bus system data (Savier & Das, 2007). 38

Table 3.4: Relay settings for conventional technique 43

Table 4.1: Comparison Table for the Goodness of Fit 47

Table 4.2: Case studies for validation of proposed technique. 49

Table 4.3: Load Priority Table for the Proposed and Adaptive Techniques. 50

Table 4.4: Load data for the Malaysian distribution system. 50

Table 4.5: Frequency Stability Parameters for Islanding event (Scenario-I). 51

Table 4.6: Frequency Stability Parameters for DG Tripping (Scenario-I). 53

Table 4.7: Frequency Stability Parameters for cascaded DG tripping. 56

Table 4.8: Load shedding parameters for IEEE 137 bus system. 58

Table 4.9: Load data for the adaptive technique. 60

Table 4.10: Frequency stability parameters for islanding event (Scenario II). 61

Table 4.11: Stability index of loads for the islanding event. 62

Table 4.12: Frequency stability parameters for DG tripping event (Scenario II). 64

Table 4.13: Stability index of load buses for DG-tripping event. 65

Table 4.14: Stability index of load buses for the overloading event............................67

Table 4.15: Frequency stability parameters for overloading (Scenario II). 68

Table 4.16: Frequency stability parameters for Islanding (IEEE 69 bus system)...........70

Table 4.17: Stability index of loads for IEEE 69-bus System. 71

Table 4.18: Frequency stability parameters for DG tripping IEEE 69 bus system.........73

Table 4.19: Load shedding parameters for the proposed scheme (islanding)................77

Table 4.20: Load shedding parameters for the proposed scheme (DG tripping). 77

LIST OF ABBREVIATIONS AND SYMBOLS

ANN	:	Artificial neural network
DG	:	Distributed generation
DFE	:	Degree of freedom for error
FVSI	:	Fast voltage stability index
GHG	:	Greenhouse gases
IEEE	:	Institute of Electrical and Electronics Engineers
ILSM	:	Intelligent load shedding module
LS	:	Load shedding
MCS	:	Monte Carlo simulation
MILP	:	Mixed integer linear programming
OLSE	:	Ordinary least square estimation
PIFM	:	Power imbalance forecasting module
PV	:	Photo Voltic
RMSE	:	Root mean square error
SI	:	Stability index
SFR	:	System frequency response
SMCS	:	Sequential Monte Carlo simulation
SSE	:	Sum of squared estimate of errors
UFLS	:	Under frequency load shedding
WLS	:	Weighted Least Square

H_i	:	Inertia constant of the i^{th} generator
M	:	Number of DGs connected in the system
N	:	Total number of loads in the system
PDG_i	:	Total dispatched power of DG_i
$MaxDG_i$	:	Maximum generation capacity of DG_i
$d(f_{sys})/dt$	:	Rate of change of the system frequency
P_i	:	Active power at bus i
Q_i	:	Reactive power at bus i
R_i	:	Resistance of bus i
X_i	:	Reactance of bus i
NCL	:	Non-critical load sets
SCL	:	Semi-critical load set
CL	:	Critical load sets
W	:	Dummy variable for MILP problem
f_n	:	Nominal frequency
SI_i	:	Stability index of i^{th} load
P_{SR}	:	Total spinning reserves
x_i	:	Load's circuit breaker status
ΔP	:	Power imbalance
PL_i	:	Real-time load value at bus i
f_i	:	Frequency of i^{th} generator

Vs_i	:	Sending end voltage for the i^{th} bus
Δ	:	Coefficient of dummy variable
α, β, and γ	:	Coefficients of the linear problem for load priority and optimization

CHAPTER 1: INTRODUCTION

1.1 Overview

Greenhouse gases (GHG) emission is a significant contributor to environmental pollution resulted in climate change. This emission is produced from various human activities, with one-third produced from electricity generation based on fossil fuels (Pan, Xu, Li, Shieh, & Jang, 2013). Such pollution is becoming more significant recently with the trend in continuous increment of electrical power demand. To minimize this emission, Distributed Generation (DG) based on renewable energy resources has great potential. The DG can be defined as *Decentralized and on-site electricity generation located contiguous to the loads from renewable energy resources*. The authors in (Davis, 2002a, 2002b) presented a comparison between central station and distributed power system considering ten different parameters. Extensive analysis of these parameters concludes that the DG is better than central station generation in terms of reliability, availability, and up-gradation.

The DGs in the distribution network can be operated in two different modes, namely, grid-connected mode and islanded mode. The DG, which shares the system load with grid supply, is stated as grid-connected mode. In this mode, the grid controls the terminal conditions, i.e., voltage and frequency. On the other hand, losing grid connection is referred as islanding of the DG. In this mode, the DG controller should isolate itself from the system within two seconds (IEEE.Standard.1547, 2003). However, the maximum benefits of DGs cannot be met if DG is always uncoupled from the system due to unstable operation. Requirements and techniques in achieving stable DG operation in islanded mode are presented in IEEE standards (IEEE.Standard.242, 2001; IEEE.Standard.1547, 2003; IEEE.Standard.94248, 2003).

DGs operating in islanding mode commonly experience an imbalance between load and generation. This happens due to total DGs capacity is lower than the total load demand in the distribution system. The difference in load demand and generation capacity, which is termed as power imbalance, destabilizes the system frequency. This may cause cascaded tripping of DGs, which yields a system blackout. Therefore, an effective solution is required to stabilize the system by minimizing the difference between demand and generation. This issue can be achieved by increasing the generation or by decreasing the system load. Since a system has certain generation limits, load shedding is inevitable to achieve a new steady-state condition by stabilizing the system's frequency (Lopes, Moreira, & Madureira, 2006).

Under Frequency Load Shedding (UFLS) techniques can be categorized into; conventional (multi-stage), semi-adaptive, and adaptive or computational intelligence-based techniques. Conventional load shedding technique is referred as shedding predefined loads from the system based on frequency threshold levels utilizing an under-frequency relay. In this technique, shedding of predefined loads can result in either excessive or inadequate load shedding. Excessive load shedding causes overshoot arising power quality issues, whereas inadequate load shedding creates instability in the system frequency, which will cause a blackout. Adaptive load shedding techniques have the advantage of estimating power imbalance separately from frequency decline rate, to disconnect predefined loads sequentially (Rudez & Mihalic, 2011). Semi-adaptive and adaptive techniques based on computational intelligence can be an acceptable substitute for conventional load shedding. Numerous techniques for semi-adaptive and adaptive load shedding have been proposed in the literature by analyzing different parameters. This approach sheds lesser loads than conventional, which results in improved frequency response.

1.2 Problem Statement

Frequency stability in power system is a major concern to utilities, especially for distribution networks when they incorporate DGs. A distribution network operating in islanding mode encounters an unbalance condition, due to the difference in demand and supply. The UFLS is inevitable to mitigate this unbalance. The UFLS schemes require accurate power imbalance estimation to shed an equivalent amount of load for optimal load shedding. Power imbalance estimation utilizing *swing equation* produces admissible results in existing techniques. However, the power imbalance estimation of the system is affected by uncertain behavior under extreme conditions and low inertia. Therefore, a new technique is required to predict an accurate power imbalance.

Accurate power imbalance estimation using computational intelligence-based techniques may not be sufficient for stabilizing the frequency of the distribution networks. Random and sequential selection of loads results in either excessive or inadequate load shedding and yields overshoot or undershoot in the frequency response. Though, some of the techniques based on exhaustive search or meta-heuristic techniques find an optimal combination of load shedding such as in (Dreidy, Mokhlis, & Mekhilef, 2017; Laghari, Mokhlis, Karimi, Abu Bakar, & Mohamad, 2015). However, computational time is too long due to large search space requirements which result in blackout before the load shedding can be executed. Therefore, an efficient technique is needed for optimal load shedding selection that will not be affected by increasing the number of loads.

Optimal selection of loads results in accurate load shedding that able to stabilize the system's frequency. However, there is a possibility of under voltage relay operation from unstable load buses before the DGs achieve steady-state operation. In order to avoid under voltage relay activation, loads from unstable buses must be shed on priority in UFLS techniques (López, Pérez, & Rodríguez, 2016; Yusof et al., 2017).

A comprehensive UFLS scheme is required to stabilize the system frequency for steady-state islanding operation of distribution network. Accurate estimation of power imbalance and selection of loads based on voltage stability index should be incorporated together for a comprehensive load shedding scheme. Furthermore, the importance level of the load must be considered while selecting the loads to be shed, since some loads are linked to a nation's economy, security, and health. Therefore, an efficient load shedding scheme is needed incorporating an optimal selection of loads considering the importance of loads and voltage stability index of loads simultaneously.

1.3 Research Objective

The focus of this research is to propose a comprehensive UFLS scheme for a distribution network operating in islanded mode. The main objectives of this research are as follows:

1) To formulate a power imbalance equation in terms of rate of change of frequency using polynomial regression.
2) To determine the optimal combination of load shedding for balancing the power using mixed-integer linear programming.
3) To rank the loads based on their voltage stability index for disconnecting more unstable loads on priority in the proposed mathematical model.

4) To integrate the proposed power imbalance equation, optimal load shedding, voltage stability index, and load priority as an effective UFLS scheme.

1.4 Research Methodology

In order to achieve the listed research objectives, the following methodologies are adopted:

1. In-depth review of the published research related to under frequency load shedding (UFLS) to propose an effective and robust approach of load shedding for an islanded distribution network.
2. Critically analyze the various techniques proposed in the literature to stabilize the system frequency.
3. Formulate the problems in existing load shedding techniques and propose a solution for these problems.
4. Classify the loads as critical, semi-critical, and non-critical to shed non-critical loads on priority ensures the functionality of critical loads.
5. Rank the loads based on their voltage stability index for prioritized selection to avoid voltage collapse at more unstable loads.
6. Study different optimization techniques for selection of loads and forecasting of power imbalance.
7. Design an intelligent load shedding module for optimized selection of loads based on mixed-integer linear programming.
8. Design a power imbalance forecasting module for accurate prediction of power imbalance in the system based on polynomial regression.

9. Simulate the proposed technique for three different test systems, i.e., 28 bus Malaysian distribution system, the IEEE 69 bus system, and the IEEE 137 bus system, to validate the robustness of the proposed study.
10. Compare simulation results with three already existing schemes in the literature to prove its superiority (Laghari et al., 2015; Yusof et al., 2017).

1.5 Scope of Research

The focus of this research is to propose a robust technique for optimal UFLS to operate a distribution network in islanding mode. The proposed technique is able to stabilize the system frequency by performing optimal load shedding. Accurate power imbalance estimation is achieved by utilizing polynomial regression, an application of machine learning algorithm. An intelligent load shedding module is proposed in this research based on Mixed Integer Linear Programming to optimize the selection of relatively more unstable loads with multiple priorities, i.e., non-critical, semi-critical, and critical. Non-critical loads are given first priority to be shed to ensure supply for critical loads. The stability of the system voltage is improved by prioritizing the loads based on their stability index so that more unstable load buses are disconnected on priority. The proposed scheme results in a smoother frequency response without any overshoot that improves power quality and reliability. The work utilizes three test systems model; 11 kV-28 bus part of the Malaysian distribution system, the 11kV-IEEE 69 bus system, and the 11kV-IEEE 137 bus system, in verifying the effectiveness of the proposed UFLS. In this work, PSCAD/EMTDC software is used for implementing and testing the proposed UFLS. The high share of non-synchronous generation sources in modern power systems presents low or no inertia. As a result, power imbalance estimation for load shedding based on the rate of change of frequency and inertia of the system may not be reliable and efficient. Hence, the proposed scheme may not work as efficiently for microgrids having only invertor based non-synchronous DGs.

1.6 Dissertation Outline

This dissertation consists of five chapters. **Chapter 1** presents an overview and background of this research. **Chapter 1** also includes problem statement, research objectives, scope, and methodology.

Chapter 2 reviews the previous works related to under frequency load shedding incorporating different mathematical and computational intelligence-based techniques.

Chapter 3 demonstrates the formulation of the proposed technique. Polynomial regression and mixed-integer linear programming optimization technique used for optimal load shedding are described in detail in this Chapter.

Chapter 4 presents the validation of the proposed technique. Comparison of simulation results with adaptive and conventional load shedding is presented in this chapter. Cumulative discussion on simulation results is explained in this chapter.

Chapter 5 presents the conclusion and future work of this research work.

CHAPTER 2: LITERATURE REVIEW

2.1 Introduction

In this modern era, the production of electrical energy is the key factor for economic development of a country. Mostly, electrical energy is produced by fossil fuels due to its reliable nature and stable supply. However, excessive use of fossil fuel causes environmental problems, mainly greenhouse gases (GHG) and CO_2. Alternatively, renewable energy resources (RES) generate emission-free electrical power and are projected to reduce GHG emissions to less than 80 percent by the year 2050 (Williams et al., 2012). Moreover, transforming conventional vehicles to emission-free vehicles that run on electricity will significantly decrease GHG and CO_2 emissions (Williams et al., 2012).

The emission of GHG and CO_2 increases the ambient temperature of the world that is called global warming. GHG emission and electricity consumption are correlated in which one-degree increment in ambient temperature due to emissions will increase per-person electricity consumption between 0.5 to 0.85 percent (Santamouris, Cartalis, Synnefa, & Kolokotsa, 2015). Emission-free electricity production from renewable energy resources and emission-free vehicles are the key factors to decarbonize the environment (Santamouris et al., 2015; Williams et al., 2012). Besides emissions, the existing power system network cannot meet the increasing demand for electrical energy. Therefore, increasing electricity demand and GHG emissions derive the attention towards the Distributed Generators (DG), especially from renewable energy resources. Moreover, DGs can decrease the transmission and distribution cost of the conventional power system by 25% (Narula, Nagai, & Pachauri, 2012; Silva, Morais, & Vale, 2012).

2.2 Limitations of DGs

Conventionally, DGs operate in grid-connected mode sharing the system load with the utility grid. It may also operate during the loss of grid, which is referred as islanding. Despite various advantages and capabilities, DGs have limitations in both operating modes. These limitations are listed in Table 2.1 and Table 2.2 (Barker & Mello, 2000).

Table 2.1: Limitations of DG in grid-connected mode

Limitation	Description
Bidirectional power flow	The voltage at the common coupling point is increased due to DGs disturbing the basic radial design of the system.
Harmonics	Electronics equipment, i.e., inverters and different control elements, create harmonics. These harmonics affect power quality significantly.
Short circuit Current	DGs in grid-connected mode impose significant changes in overall fault current levels.

Table 2.2: Limitations of distributed generation in islanded mode

Limitation	Description
Voltage and frequency stability	Power imbalance in islanding condition overloads the DGs resulting unstable voltage and frequency, that effects the customers (Azmy & Erlich, 2005)
Transients in inertia	Penetration of inverter type DGs introduce variable inertia and produce transients during standalone operation (Meegahapola & Flynn, 2010)
Cascaded blackout	Power mismatch overloads the system and influences the cascaded DG tripping due to low frequency.

2.3 Under frequency load shedding

Islanding commonly creates a power imbalance in the system as total load demand is higher than the total generation that affects the stability of the system's frequency. Unstable frequencies result in a blackout due to cascaded tripping of DGs due to under frequency protection. Therefore, under frequency load shedding (UFLS) is required to mitigate the power imbalance (Lopes et al., 2006). UFLS has been investigated extensively in the literature recently with the integration of DGs in modern power systems. The existing UFLS techniques can be categorized as conventional, semi-adaptive, adaptive, and artificial intelligence-based techniques.

2.4 Conventional under frequency load shedding

Conventional load shedding incorporating under frequency relay is the earliest technique for frequency stability. UFLS started with the invention of under-frequency load shedding relay way back in 1971. Later on, with the advancement, this relay went through improvements and was considered a good option for restoration of the system by shedding different predefined loads at certain threshold levels. Various studies yielded different types of relays that are capable of shedding loads at certain limits (Anderson & Mirheydar, 1992; Girgis & Ham, 1982; Taylor, 1992).

Conventional load shedding became the trend for a power system with the dominance of DG in the power system. Several researchers' work was based on this technique. In (Jiang, Yan, Ji, Liu, & Shan, 2010), a technique is proposed to dynamically change the frequency relay setting during the steps of load shedding. The authors claimed that the proposed method sheds lesser loads than the conventional relay. The system starts shedding the load when the frequency reaches a threshold of 49Hz in steps of 0.3 pu load. Although this effort introduced a new path to stabilize the system frequency, it has significant drawbacks to be a reliable technique. Load shedding without priority, sequential load selection, and predefined threshold levels produce overshoot in the frequency response.

The frequency response has been used frequently in different models to improve the frequency stability of the system. Basic load shedding necessary to operate a system after any disturbance is explained in (Ford, Bevrani, & Ledwich, 2009). Load shedding was designed based on local frequency response using spinning reserves, and the frequency relays operate in steps of 0.2 pu load depending on frequency thresholds, i.e., 49.75Hz, 49.5Hz, and 49.25Hz. Shared load shedding for an interconnected system of the different regions is also presented in (Ford et al., 2009). The major drawback of conventional load shedding scheme is excessive load shedding.

The inertia of the system opposes the sudden change in frequency; therefore, the frequency further declines after the load shedding and then starts to stabilize back. This decline in frequency is defined as frequency nadir. This frequency nadir activates an additional load shedding step according to predefined threshold level and causes a significant overshoot in frequency. Predefined frequency threshold levels require an adaptive change to avoid unnecessary activation of load shedding steps.

2.5 Semi-Adaptive under frequency load shedding schemes

Semi-adaptive techniques were improvement of the conventional load shedding techniques because they only shed an equivalent load from the system to minimize the power imbalance. Under frequency relay settings are dynamically changed in these techniques to improve the frequency response. Various techniques for semi-adaptive load shedding have been proposed in the past. The second derivative of frequency response has been used to improve the frequency stability of the system in a multi-step load shedding scheme (Rudez & Mihalic, 2011). The focus is to stop the frequency falling below 47.5 Hz. Newton method based approximation is used to forecast the minimum frequency. Load shed amount for each step is estimated from this minimum frequency value. The proposed technique can only be considered as updated under frequency relay as the loads were shed in multiple steps without priority, and no dynamic relay setting for frequency nadir was defined.

A new physical relay that can work for UVLS and UFLS simultaneously for a given system has been proposed in (Ye, Baohui, Zhiqian, & Junzhe, 2015) to disconnect different loads in multiple steps to maintain the parameters within the limit. A new steady-state condition in 15 to 30 seconds is achievable using this relay. However, the time required to achieve a new steady-state condition endangers the turbine stability as the turbine blades may damage due to operating in unstable frequency region for a longer duration of 15 s. In a related study (Haes Alhelou, Hamedani-Golshan, Njenda, & Siano, 2019), the system frequency response identified from the phasor measurement units are introduced to form a new multistage load shedding scheme. However, the availability of latest synchrophasor measurement units may not be possible for all power systems, thus challenging the robustness of the scheme. Moreover, loads have been shed without priority and sequentially, which may result in unoptimized frequency response.

Another UFLS technique based on Lagrange multipliers, proposed in (Gautam, Bhusal, & Benidris, 2020), estimates the load shedding steps by analyzing the power deficit and optimizes the load shedding location. However, numbers of load shed were chosen arbitrarily, and that raises concerns regarding the vulnerability of this technique. Moreover, pre-determined frequency thresholds and sequential selection of loads hinder the accuracy of such techniques, resulting in a frequency overshoot due to the excessive load shedding. On the other hand, linear programming has been employed to minimize the load shedding amount for each step in a multistage load shedding scheme (Potel, Debusschere, Cadoux, & Rudez, 2019). This technique optimizes the frequency threshold level after each load shedding step, and relay settings are updated dynamically. In this technique, pre-determined loads are shed sequentially, which lead to either excessive or inadequate load shedding. Moreover, loads are not given any priority, which may yield a disconnection of critical load.

Excessive load shedding causes power quality related problems (voltage and frequency instability). Meanwhile, inadequate load shedding will lead to a blackout of the system. Thus, adaptive settings for under frequency relay is proposed in (Rafinia, Moshtagh, & Rezaei, 2020). This technique optimizes the frequency setpoint, time delay, and load shed amount for each step that is incorporated in mixed-integer linear programming. Although the proposed load shedding technique minimizes the load shed amount and frequency is in permissible range of 49.5-50.5 Hz, mostly the frequency stability is at risk due to inadequate disconnection of loads. Conversely, computational intelligence-based applications are gaining attention. Hence, proposing new schemes based on computational intelligence techniques may result in better and improved frequency response. A comparison of the limitations and advantages of all the semi-adaptive techniques are summarized in Table 2.3.

2.6 Intelligent under frequency load shedding

The swing equation linearly correlates the mechanical and electrical power of a generator (Caliskan & Tabuada, 2015). However, Zhou *et al.* (J. Zhou & Ohsawa, 2009) found that this correlation is not valid for extreme and rapidly varying loading conditions. Due to limitations in power imbalance estimation, researchers also explored the application of artificial intelligence techniques for load shedding purposes. These techniques have advantages in solving a non-linear problem with better efficiency. Artificial intelligence-based techniques can measure and predict power imbalance more precisely if sufficient data on the behaviour of the system is available.

Table 2.3: Comparison of semi-adaptive LS techniques

Reference	Technique/Method	Advantage	Limitation
Rudez & Mihalic, 2011)	Second derivative of frequency and Newton method-based approximation	Load shed amount for each step is updated after the initial step	Can only be considered updated frequency relay Frequency threshold is set very low
Ye, Baohui, Zhiqian, & Junzhe, 2015	A new UVLS and UFLS relay	Simultaneous Voltage and frequency stability	Time taken to achieve new steady-state condition is very high
Haes Alhelou, Hamedani-Golshan, Njenda, & Siano, 2019	Phasor measurement units	Intelligent multi-level load shedding	Availability of synchrophasor measurement units, Sequential load shedding without priority
(Gautam, Bhusal, & Benidris, 2020	Lagrange multipliers based UFLS technique	Power deficit estimation for each step	pre-determined frequency thresholds and sequential selection of loads
Potel, Debusschere, Cadoux, & Rudez, 2019	linear programming	Dynamic update for frequency relay settings	Load priority is absent Small test system for validation
(Rafinia, Moshtagh, & Rezaei, 2020	Mixed-integer linear programming	adaptive settings for under frequency relay	Inadequate load shedding Missing load priority

2.6.1 Intelligent LS schemes based on ANN

Artificial neural network (ANN) is the first intelligent technique used to improve load shedding as in (Hooshmand & Moazzami, 2012), where an adaptive technique for UFLS using ANN is proposed. Power generation P_g, active power load P_i, total spinning reserves, and frequency decline rate has been selected as inputs to the ANN. With sufficient training data, the proposed ANN model was able to provide a suitable output to shed lesser loads than the conventional techniques in steps of 10%, 20%, and 25% of total load with 0.1 seconds of delay in each step. Although this technique opened up a new path for the UFLS technique, it is only improvement shape of UFLS relay with intelligent control and settings. In (Athila Quaresma Santos, Monaro, Coury, & Oleskovicz, 2014), a new technique of load shedding is presented using ANN with two inputs (instantaneous and average rate of change of system frequency) with the output is the active Power imbalance between generation and demand. The system consists of one generator and loads of five feeders. The calculated power-imbalance equivalent load is shed from the system using the relay setting. However, since the test system is a very small scale with only five buses, its effectiveness for a large system is questionable. In (Yan, Li, & Liu, 2017) adaptive load shedding is presented using ANN to measure power imbalance for 36 bus system having eight machines and load frequency regulation factor is considered to shed different loads for each bus. In this work, loads were selected randomly without any consideration of their importance.

With so much research in optimization techniques, hybrid techniques are another best option besides the stand-alone techniques for optimization. Such a technique has been applied for UFLS in (Moazzami, Khodabakhshian, & Hooshmand, 2015). In this work, ANN and a hybrid culture-particle swarm optimization- co-evolutionary algorithm were applied. The proposed scheme applied to IEEE 118 bus system and performs better and faster than conventional schemes. It also calculates the active as well as reactive power to be shed in each pre-defined step. However, load shedding's priority is not considered in disconnecting the loads. Random selection may cause a critical load to be selected.

2.6.2 Intelligent LS schemes based on Fuzzy logic

Fuzzy logic is the other popular technique used in load shedding. A Fuzzy-based load-shedding scheme for a small university distribution system has been implemented in (Çimen & Aydın, 2015), where the system has one PV plant and six small generators. For proper functioning of the system at peak demand, load shedding is necessary to provide uninterrupted supply to critical areas, for example, surgery unit. The fuzzy controller has two inputs (1-daily PV output and daily load demand) and one output (load to be shed). Although this technique produces admissible results for a specific application, an optimal solution for a general system and large-scale implementation is missing. UFLS based on

Fuzzy logic has also been tested for a steam-driven sugar industry plant (Khezri, Golshannavaz, Vakili, & Memar-Esfahani, 2017). Steam input deviation and frequency deviation have been considered as the inputs and two-layer outputs deciding load clusters, and a number of loads are the outputs. The proposed method sheds fewer loads than conventional UFLS and stables the frequency at a nominal value. The main limitation of fuzzy logic to be a reliable UFLS technique is the need to update the membership function for different test systems.

Forecasting power imbalance using ANN (Hooshmand & Moazzami, 2012; Moazzami et al., 2015; Athila Quaresma Santos et al., 2014), distribution state estimator (Karimi, Wall, Mokhlis, & Terzija, 2017) and fuzzy logic (Çimen & Aydın, 2015; Khezri et al., 2017) anticipate a more accurate power imbalance. However, in these works, load shedding was executed in a conventional approach without prioritizing loads, which results in excessive or inadequate load shedding. Moreover, practical implementation of these AI-based adaptive techniques is still questionable as compared to semi-adaptive and adaptive techniques (Laghari, Mokhlis, Bakar, & Mohamad, 2013). The conventional approach for load selection and limited practical applications for these intelligent techniques suggests that mathematical relation (swing equation) based estimation of power imbalance and intelligent load selection will result in a better load shedding approach.

2.7 Adaptive under frequency load shedding

Estimating power imbalance in islanded system from frequency decline information and shedding the equivalent amount of load from the system can be classified as adaptive load shedding technique. A load shedding scheme for Malaysian distribution network with event-based and response-based strategies has been proposed in (Karimi, Mohamad, Mokhlis, & Bakar, 2012). The power imbalance is calculated using the rate of change of frequency information and inertia of the system. Equation (2.1) is known as Swing-equation, which uses this information and estimates the power imbalance of the system.

$$\Delta P = \frac{2*\sum_{i=1}^{N} H_i}{f_n} X \ \frac{d(f_{sys})}{dt} = \ \sum_{i=1}^{N}(P_{mi} - P_{ei}) \qquad (2.1)$$

Where f_n is nominal frequency of the system, H_i is inertia constant of i^{th} generator, f_{sys} is system frequency, P_{mi} is mechanical power of i^{th} generator and P_{ei} is electrical power of i^{th} generator. Swing equation calculates power imbalance in the system, and loads are selected sequentially by load shedding controller module. The sequential selection of loads results in excessive load shedding.

Another load shedding technique based on multi-objective function also has been proposed in the past. Three objective functions, *i.e.,* minimum load shedding, loads priority, and minimum points to cut the loads, are proposed in (Wang, Guo, Wu, Liu, & Zhou, 2014). However, the test system used to verify the proposed method is small, *i.e.,* IEEE 9 bus system. Thus, the effectiveness of the proposed method is not properly validated. Furthermore, loads shed were selected randomly without assessing the nature of the loads and stability index.

A multi-agent single-stage load shedding scheme based on a multi-hierarchical centralized control structure is proposed in (Athila Quaresma Santos, Monaro, Coury, & Oleskovicz, 2019). This research calculated the power imbalance from the real-time load and generation data from advanced household devices. Then, it sequentially shed the necessary loads in a single step to restore the system. The availability of these devices and the sequential selection of loads are the major concerns regarding this UFLS technique.

Another similar approach towards load shedding is proposed in (Qing, Shicong, Jun, & Guangquan, 2016), considering the installation of advanced household devices. These advanced devices are capable of transmitting the voltage and frequency information to the master control center continuously. Master control center receives the information from the devices to act for the disturbances accordingly. However, the availability of these advanced control devices is a major challenge.

In (Q. Zhou, Li, Wu, & Shahidehpour, 2018), a new UFLS technique is proposed. Load shedding is divided into two steps. The first step is utilized to achieve a temporary stable frequency using primary control and battery energy storage system. Secondary control solves and stabilizes the system at a reliable steady-state condition using the proposed new algorithm. The proposed technique lacks accurate load shedding selection, and load priority and protection control have also been ignored in this two-step load shedding.

A new regionalization-based load shedding scheme is proposed in (Nourollah, Aminifar, & Gharehpetian, 2018). Depending upon the different contingencies, load regions and a master bus for each contingency are defined for a European interconnected system. Using loading information, the system is stabilized by shedding loads starting at most sensitive buses for that contingency. This technique was again a system-specific, and the effectiveness of the technique is not validated for a general distribution system, which may not have the advance control devices. A comparison of advantages and limitations for discussed adaptive techniques is presented in Table 2.4.

Researchers tried to explore different parameters and techniques to stabilize the system frequency to get an optimal solution for frequency stability problems. Location and type of disturbance and load have a significant effect on system stability and load shedding, which was not investigated in the techniques discussed above. Shedding non-critical loads first to ensure supply availability for critical loads will undoubtedly improve the reliability of a power system. Furthermore, the stability index of load busses must be given consideration to avoid operation of under-voltage relays for a reliable UFLS technique.

Table 2.4: Comparison of adaptive LS techniques

Reference	Technique/Method	Advantage	Limitation
(Karimi, Mohamad, Mokhlis, & Bakar, 2012	Event and response-based load shedding scheme	Estimate power imbalance and shed equivalent load in a single step	Sequential and random load selection without optimizing
Wang, Guo, Wu, Liu, & Zhou, 2014	Multi-objective function	Minimum load shedding and minimum points to cut the loads	Very small test system, i.e., IEEE 9 bus system
(Athila Quaresma Santos, Monaro, Coury, & Oleskovicz, 2019	A multi-hierarchical centralized control structure	multi-agent single-stage load shedding scheme	• Availability of advance household devices • Sequential load selection
(Qing, Shicong, Jun, & Guangquan, 2016	installation of advanced household devices	Improved frequency response	Availability of advance household devices
Q. Zhou, Li, Wu, & Shahidehpour, 2018)	Two-step load shedding to avoid transients	Introducing battery storage	Conventional load selection.
Nourollah, Aminifar, & Gharehpetian, 2018)	Regionalization-based load shedding	Load shedding scheme for a practical European interconnected system	• Availability of advance control devices • System-specific load shedding scheme

2.7.1 Adaptive LS schemes based on voltage stability index

The position of disturbance for the same power mismatch results in different disturbance scale of transient voltages at different buses. The location of disturbance alters the scale of disturbance for different loads. The type of disturbance also plays a vital role in finding the new steady-state condition for the same power mismatch (Reddy, Chakrabarti, & Srivastava, 2014).

Simulations for IEEE 39 bus system show that fewer loads are shed for the same power mismatch with the additional advantage of improved voltage stability at new steady-state conditions quickly (Li & Zhang, 2014).

Prioritized selection of non-critical or more unstable loads is a better alternative to the conventional approach of sequential selection. The research in under-frequency load shedding techniques evolves with the consideration of load priority in load shedding. Work in (López et al., 2016) proposed load shedding priority based on Fast Voltage Stability Index (*FVSI*) as in (2.2).

$$FVSI = \frac{4Z_{ij}^2 Q_r}{V_s^2\, X_{ij}} \tag{2.2}$$

Where V_s is sending voltage, Z_{ij} is the impedance of the line *i-j*, Q_r is a reactive load at receiving end, X_{ij} is reactance of the line *i-j*. FVSI is calculated for each bus and arranged in descending order to shut the loads one by one until all the buses achieve a new steady-state voltage between 0.85-1.00 pu. However, the stability of the system frequency has not been investigated explicitly. It is assumed that frequency is recovered when the system voltage is stabilized, which endangers the frequency stability.

A new stability index called RoCoFL index is proposed in (Mohammadi-Ivatloo, Mokari, Seyedi, Ghasemzadeh, & Engineering, 2014) with few improved parameters for the technique. This method is tested for the 14-bus Danish system. This technique of prioritizing the loads based on their voltage stability increases the reliability of the protection system. Un-necessary under-voltage protection activation is avoided by disconnecting unstable loads on priority. Another UFLS technique has been proposed in (Mokari-Bolhasan, Seyedi, Mohammadi-ivatloo, Abapour, & Ghasemzadeh, 2014), using load priority by considering RoCoF of load indices updated every few minutes to cover for the load variation effect. In this technique, the customer's willingness to pay is also considered in the load priority table. Frequency relays are used to continuously send the local frequency to master control where the amount of load shed is determined. A weak disturbance event for which no load shedding is required is also introduced using a new variable m_o, defined as "the change in frequency that can be stabilized using spinning reserves of the system." All the simulation for this technique is implemented on the 14-bus Danish system having wind turbine generators and CHP. The objectives for an adaptive load shedding technique are to minimize the load shed amount and prioritized the selection of unstable loads. However, a small test system for validation and sequential selection of loads are the major drawbacks of these techniques.

The stability index of loads for different disturbances is a vital factor; a study in (A. Q. Santos, Shaker, & Jørgensen, 2018) showed that prioritization of loads utilizing fuzzy logic considering social, economic, or political aspects of connected loads could further improve the reliability. Estimation of stability indices of loads (Yusof et al., 2017) to prefer unstable loads for shedding results in an improved voltage profile of the system, avoiding the operation of under-voltage protection. The relation used to calculate the stability index in this technique is presented in Equation (2.3).

$$SI_i = \left(Vs_i\right)^4 - 4\left[\left(P_i.X_i - Q_i.R_i\right)^2 - 4\left(P_i.R_i - Q_i.X_i\right)^2\right].\left(Vs_i\right)^2 \qquad (2.3)$$

Where SI_i is stability index of bus i, Vs is sending end voltage for bus i, P and Q are active and reactive powers respectively, R is resistance of the line and X is the reactance of the line. However, sequential selection of loads arranged in ascending order with respect to stability index in (A. Q. Santos et al., 2018; Yusof et al., 2017) results in frequency overshoot due to excessive shedding, despite prioritizing the loads. Therefore, finding an optimal combination of loads to be shed incorporating load priority, is an alternative approach to sequential selection.

2.7.2 Adaptive LS schemes based on optimal load selection

Smoother frequency response can be achieved by selecting a load combination that exactly matches an estimated power imbalance. Exhaustive search tool proposed in (Laghari et al., 2015) finds the best optimal combination that exactly matches with power imbalance in the system from a set of variable loads. Exhaustive search can discover load combinations; however, increasing the number of loads for a large-scale system will increase computation time and complexity of the task due to the large search space requirement. It is infeasible to execute all 2^n combinations (where *n* is the total number of loads in the test system). The possible combinations for the IEEE 69 bus system will be around 281 trillion, a physical memory space required to store and evaluate such combinations is unreal and infeasible in practical scenarios.

Another load shedding technique based on meta-heuristic techniques also exists in literature (Dreidy et al., 2017). This technique finds the best combination of loads that exactly matches the power imbalance in the system using meta-heuristic techniques. However, an increased number of possible combinations will increase the convergence time. The system may collapse before the convergence due to cascaded tripping of DGs with unprecedented frequency variations. From the above analysis of UFLS schemes, it is revealed that an optimal technique to find a combination of loads that exactly matches the estimated power imbalance is still needs to be explored, which is not affected by the increase in the number of loads and possible combinations.

2.8 Summary

Successful islanding operation of a distribution system with a different type of DGs is the aim of all the discussed methods. The operation of a distribution system in islanding requires a balance of demand and supply. Frequency tends to decrease whenever there is a mismatch of total load and total generation, with load more than generation. Load shedding is unavoidable to stabilize the system frequency and mitigate the difference in demand and supply. Therefore, an intelligent load shedding technique is needed that can achieve a new steady-state condition in minimum time with a maximum load connected to avoid a blackout and maximize the benefits from DG.

Detaching predefined loads from the system through an under-frequency relay based on frequency threshold levels is described as conventional load shedding. Dynamically updating the under-frequency relay settings for load shedding is classified as semi-adaptive load shedding. Incorporating computationally intelligence-based techniques for load shedding is defined as intelligent load shedding. Sensing and calculating the power shortage in the system and disconnecting loads optimally from the system is referred as adaptive load shedding. This chapter illustrates different load shedding schemes to analyze and formulate the shortcomings in these techniques. Different intelligent computational based techniques have been proposed in the literature to forecast power imbalance accurately and shed lesser loads. However, the optimal selection of loads has not been studied extensively to minimize the load shed amount and avoid overshoot or undershoot in frequency response. Moreover, prioritized selection of non-critical and more unstable loads will increase the reliability of the system and functionality of critical loads will not be affected. Considering all the aspects discussed above, a new UFLS scheme is offered in this research. The feasibility of the proposed scheme for practical implementation is analysed through dynamic analysis in PSCAD/EMTDC software. The main contributions of this research are:

1. Accurate forecasting of power imbalances for any contingency in the system using polynomial regression.

2. The reliability of the system is increased by prioritized selection of non-critical loads to ensure supply to semi-critical and critical loads, although load shedding initiated.
3. The stability of the system voltage and frequency is improved by prioritizing the loads based on their stability index so that more unstable load buses are disconnected on priority.
4. Mathematical modelling-based strategy for optimal selection of loads from unstable and non-critical loads to be shed using MILP to improve frequency response with minimum frequency overshoot during islanded operation of distribution system connected with DGs.

CHAPTER 3: PROPOSED UNDER FREQUENCY LOAD SHEDDING

3.1 Introduction

This research aims to propose a new UFLS technique that yields an optimal solution for the frequency stabilization of an islanded distribution system. The working principle of the proposed technique is explained in a block diagram shown in Figure 3.1. The proposed technique in this research comprises four modules:

1) Average system frequency calculation module
2) Power imbalance calculation module
3) Stability index calculation module
4) Intelligent load shedding module

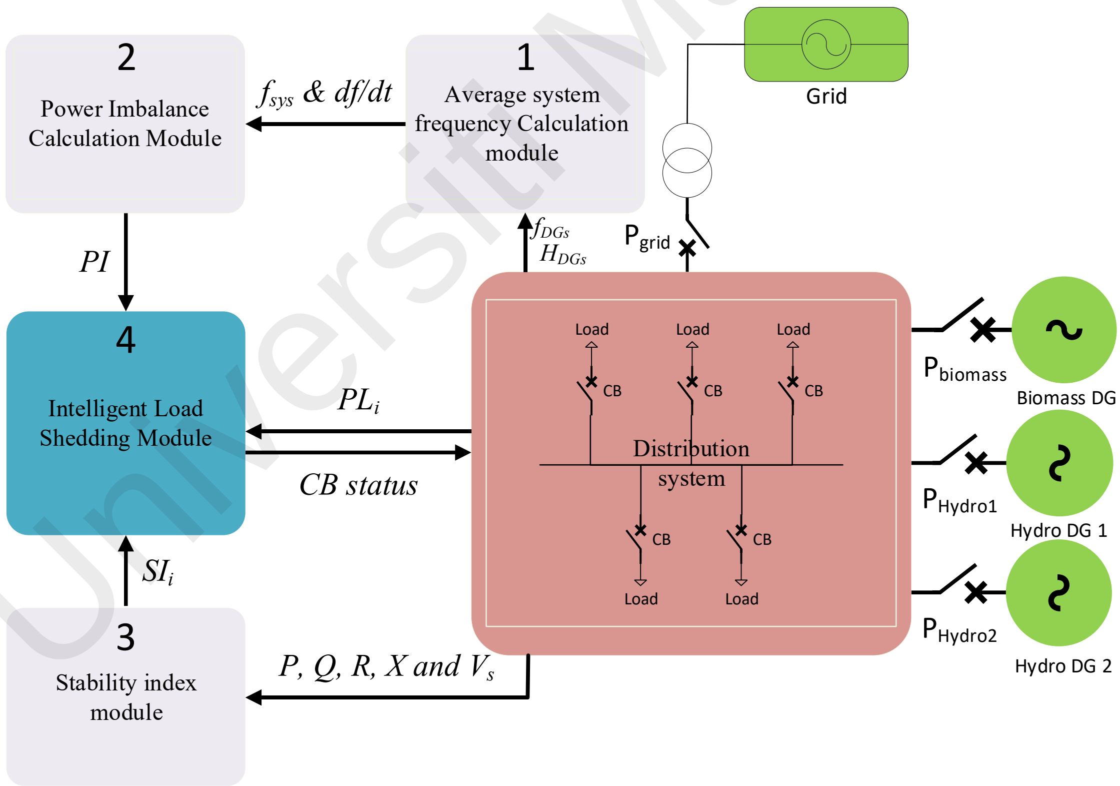

Figure 3.1: Block diagram of the proposed load shedding scheme.

The working of all the above modules is explained in the following sections.

3.2 Average System Frequency Calculation Module

The basic parameter of any load shedding scheme is frequency. In grid-connected mode, the grid controls the system frequency with DGs supplying power to some of the load. However, in islanded mode, the system frequency will behave abnormally due to drastic changes in generation and load balance. Furthermore, the inertia constant, spinning reserve, and turbine control mechanism of each DG further alter the system frequency. Thus, an average system frequency needs to be considered during islanded mode as in Equation (3.1):

$$f_{sys} = \frac{\sum_{i=1}^{M} H_i \cdot f_i}{\sum_{i=1}^{M} H_i} \tag{3.1}$$

,where H_i is the inertia constant of the i^{th} generator in seconds, f_i is the frequency of the i^{th} generator, and M is the number of DGs connected in the system. The rate of change of system frequency is evaluated from the derivative of f_{sys}. This decaying frequency information is used to calculate the power imbalance in the system.

3.3 Power imbalance forecasting module (PIFM)

It is very important to estimate power imbalance as accurate as possible so that the correct amount of load shed can be executed. By shedding a load amount equal to the imbalance power, a smooth frequency recovery can be achieved. A well-known method to estimate the power imbalance from the severity of frequency is based on swing equation (Dreidy et al., 2017; Laghari et al., 2015). In this equation, the power imbalance is in the form of rate of change of frequency. Therefore, it is possible to create a power imbalance equation as a function of the rate of change of frequency. In (J. Zhou & Ohsawa, 2009), Zhou *et al.* found that a higher-order non-linear equation can present the relation between mechanical power and electrical power more accurately, especially for variable loading conditions in low inertia distribution systems. Taken the same idea, in this study, a correlation between the independent variable (rate of change of f_{sys}) and the dependent variable (ΔP) is predicted using regression analysis. The equation from the regression is used in the proposed PIFM module. Polynomial regression predicts the values for the ΔP by utilizing ordinary least square estimation. The smaller difference between predicted and actual ΔP, yields for a better fitting of data. Simple relation between the regressor and the estimator is shown in Equation (3.2).

$$\Delta P = \alpha_0 + \alpha_1 X + \alpha_2 X^2 + \cdots \alpha_m X^m + \varepsilon \tag{3.2}$$

$$X = \frac{d(f_{sys})}{dt} \tag{3.3}$$

,where ΔP is the power imbalance, m is the degree of the polynomial used for regression, $\alpha_o, \alpha_1, \alpha_2, \ldots \alpha_n$ are the coefficients of the polynomial, X is the rate of change of the frequency, and ϵ is the random error factor. The polynomial regression analysis was first carried out for different conditions and constraints in the test system. While considering numerous input variations and various possible scenarios in the system, the collected output data was then used for further analyses. The polynomials and the computation of the coefficients for the polynomial variables were executed based on the following mathematical expressions (3.4) and (3.5).

$$\begin{bmatrix} \Delta P_1 \\ \Delta P_2 \\ \vdots \\ \Delta P_n \end{bmatrix} = \begin{bmatrix} 1 & X_1 & X_1^2 & \cdots & X_1^m \\ 1 & X_2 & X_2^2 & \cdots & X_2^m \\ \vdots & \vdots & \vdots & \ddots & \vdots \\ 1 & X_n & X_n^2 & \cdots & X_n^m \end{bmatrix} \begin{bmatrix} \alpha_0 \\ \alpha_1 \\ \vdots \\ \alpha_n \end{bmatrix} + \begin{bmatrix} \varepsilon_1 \\ \varepsilon_2 \\ \vdots \\ \varepsilon_n \end{bmatrix} \tag{3.4}$$

$$\overrightarrow{\Delta P} = \vec{X}.\vec{\alpha} + \vec{\varepsilon} \tag{3.5}$$

,where n is the total number of input and output values. The estimated polynomial regression coefficient vector was calculated using an ordinary least square estimation based on Equation (3.6).

$$\vec{\alpha} = (X^T X)^{-1}.X^T \overrightarrow{\Delta P} \tag{3.6}$$

The elements of the coefficient matrix were finally used in (3.3) to estimate the power imbalance in the system. Then, a threshold level of the power imbalance was set to prevent unnecessary load shedding. The threshold level standard for load shedding activation is taken as the smallest load in the system. If the power imbalance calculated by this module is more than the threshold value, the PIFM module estimates the load shed amount incorporating spinning reserves of DGs, as shown in Equation (3.7).

$$PI = \Delta P - P_{SR} \tag{3.7}$$

,where PI is the load shed amount, and P_{SR} is the total spinning reserves in the system. Spinning reserves can be calculated by Equation (3.8)

$$P_{SR} = \sum_{i=1}^{M} MaxDG_i - \sum_{i=1}^{M} PDG_i \tag{3.8}$$

,where $MaxDG_i$ is the maximum generation capacity of i^{th} generator, and PDG_i is the total dispatched power of *the* i^{th} generator. This PIFM can monitor all the changes in the system. The working of the proposed PIFM module is explained in a flow chart in Figure 3.2.

In the case that the power imbalance is more than the set threshold level, the load shed amount calculated using Equation (3.8), will be passed over to the intelligent load shedding module (ILSM) for shedding of an equivalent amount of load. Moreover, this module will transmit an activation signal to the stability index calculation module (SICM) to estimate the stability indices of load buses.

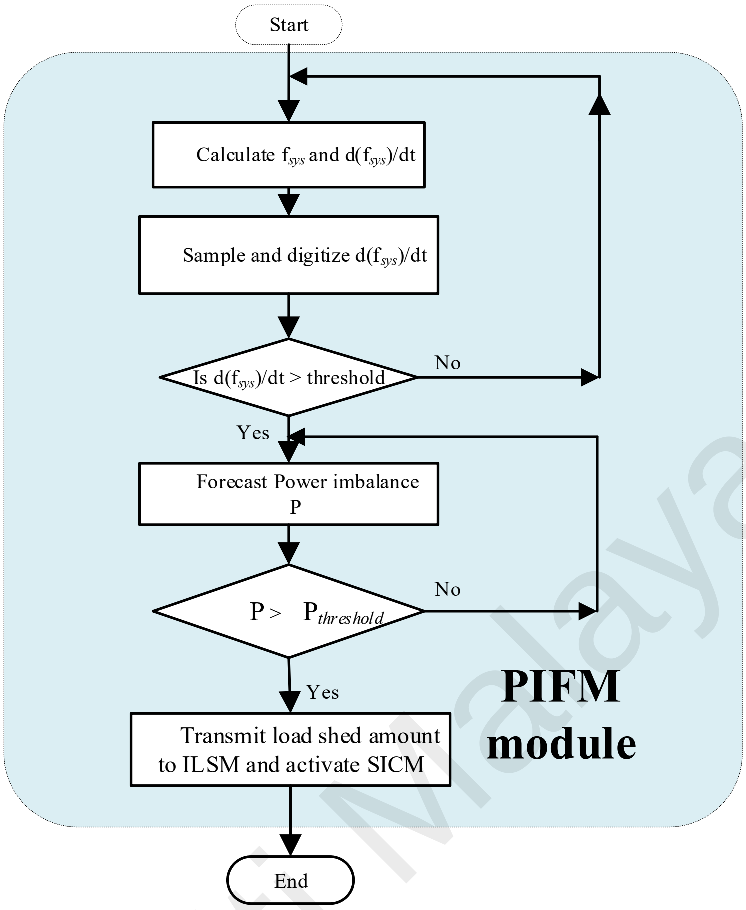

Figure 3.2: Flow chart of the proposed PIFM module.

3.4 Stability Index Calculation Module (SICM)

The stability index of a bus in a distribution system depends upon the connected load and the sending end voltage to that bus. Furthermore, it also depends upon the impedance of that distribution line (Chakravorty & Das, 2001). This module will capture real-time sending end voltage, load, and impedance values of each bus when the activation signal from the PIFM is received. The stability index for this scheme is calculated using Equation (3.9), which was proposed in (Chakravorty & Das, 2001) and utilized for load shedding in (Yusof et al., 2017).

$$SI_i = \left(Vs_i\right)^4 - 4\left(P_i.X_i - Q_i.R_i\right)^2 - 4\left(P_i.R_i - Q_i.X_i\right).\left(Vs_i\right)^2 \quad (3.9)$$

where SI_i is the stability index of the i^{th} load bus, P_i, Q_i, R_i, X_i, and Vs_i are active power, reactive power, resistance, reactance, and sending end voltage, respectively, for the i^{th} bus. The stability indices calculated in this module are then transmitted to the ILSM for activating optimal load shedding selection.

3.5 Intelligent Load Shedding Module (ILSM)

The ILSM provides an optimal solution for load shedding, where it captures the real-time load values from PSCAD software. These loads have been categorized as non-critical, semi-critical, and critical loads. The power imbalance forecasted in the PICM is analyzed, and a combination of loads for shedding if the power imbalance is greater than $P_{threshold}$ is determined by solving the MILP optimization. The proposed MILP model and objective function of the problem are shown in canonical form, Equation (3.10) is the objective function, Equations (3.11) and (3.12) are constraints to follow, and Equations (3.13) and (3.14) present parameter limits.

$$OF = \min \sum_{j \in NCL} \alpha.SI_j.x_j + \sum_{k \in SCL} \beta.SI_k.x_k + \sum_{l \in CL} \gamma.SI_l.x_l + \delta.w \qquad (3.10)$$

Subject to

$$\sum_{i=1}^{N} (x_i.PL_i) - w \le PI \quad \forall PL_i \ge 0 \qquad (3.11)$$

$$\sum_{i=1}^{N} \{x_i.(-PL_i)\} - w \le (-PI) \quad \forall PL_i \ge 0 \qquad (3.12)$$

$$\alpha, \beta, \gamma \quad and \quad \delta \quad are \quad non \quad negative \quad numbers \qquad (3.13)$$

$$x_i = \begin{cases} 0 & Disconnected \\ 1 & Connected \end{cases} \quad \forall i = 1, 2, 3 \cdots N \qquad (3.14)$$

,where PL_i is the real-time load value at bus i, N is the total number of loads in the system, SI is the stability index of the load, NCL, SCL, and CL are noncritical, semi-critical and critical load sets, respectively. The binary variable x takes a value of 1 if the load's circuit breaker disconnects the load from the system, 0 otherwise. α, β, and γ are coefficients of the linear problem for load priority and optimization. These values are calculated so that the model should not select any additional semi-critical or critical load and only shed the non-critical loads. The objective function is to minimize the difference of the estimated power imbalance, and ideally, it should be 0. However, it cannot be 0 for all possible scenarios. Therefore, a dummy variable is needed to satisfy the designed constraints in certain conditions. The variable w in the objective function is a dummy variable, and δ is its coefficient. Its coefficient δ is given a very high value so that the objective function minimizes this dummy variable value. The block diagram of this module is shown in Figure 3.3.

This module finds the optimal combination of loads to be shed to match the power imbalance of the system with minimum error, incorporating stability indices of loads and load priority. The following conditions are performed during the load shedding process:

1. A combination of only non-critical and more unstable loads will be shed if the power mismatch is less than the total non-critical load in the system.
2. If the power mismatch is more than the total amount of non-critical loads in the system, the module will shed an optimal combination of more unstable non-critical and semi-critical loads to match the power imbalance in the system. However, non-critical loads will be shed on priority.
3. Lastly, if the power imbalance is more than the amount of non-critical plus the semi-critical loads, all the non-critical and semi-critical loads will be shed, and an optimal combination of critical loads will be determined for balancing the load and supply. It is a better option to disconnect a few of the critical loads instead of total blackout in case of extreme contingency.

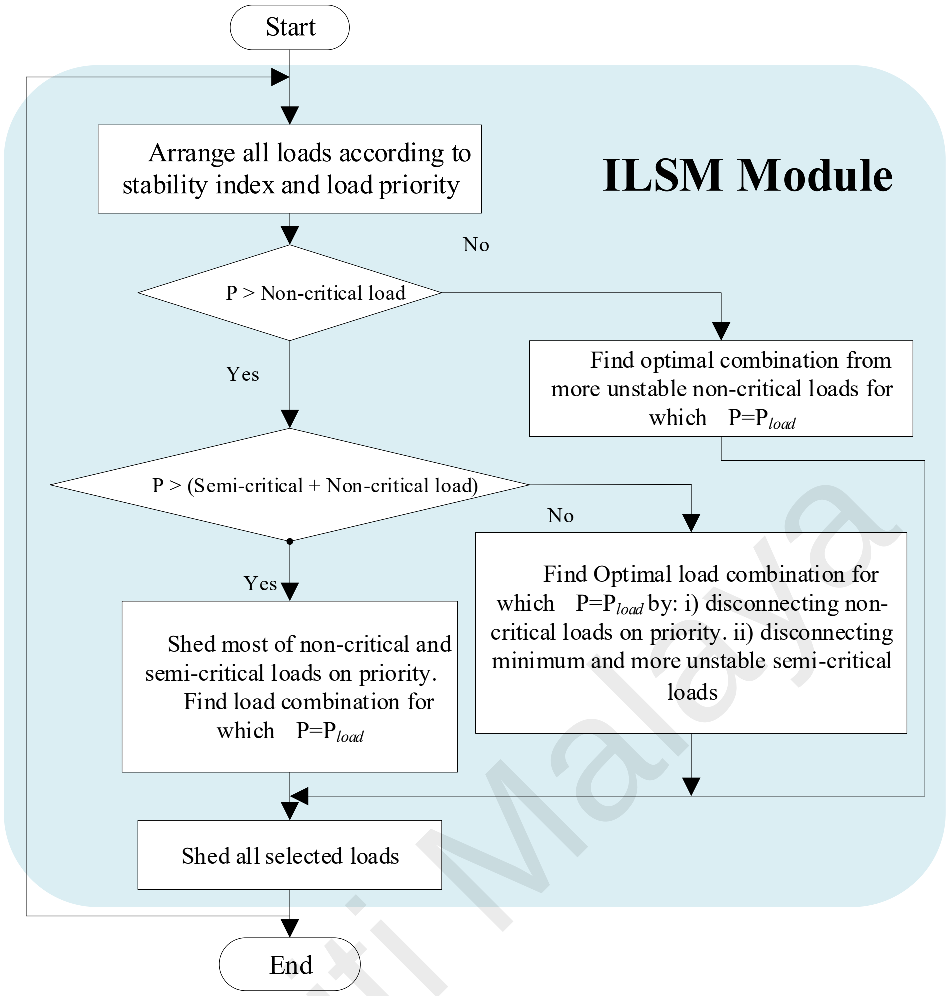

Figure 3.3: Flowchart of the proposed intelligent load shedding module (ILSM).

3.6 Test System modeling

The efficacy of the proposed study is validated on three different test systems, i.e., 28 bus practical system that is part of the Malaysian distribution network, the IEEE 69 bus system, and the IEEE 137 bus system.

3.6.1 Malaysian 28 bus distribution system

This system is part of the Malaysian 11 kV distribution network. It comprised three DGs, of which two DGs where mini-hydro generators and one a bio-mass generator, coupled with the grid supply and 20 lumped loads. Each DG is rated at 2 MVA at a voltage level of 3.3 kV. The maximum dispatch capacity is 1.82 MW for each of hydro DGs and 1.86 MW for the bio-mass DG. A single line diagram of this system is shown in Figure 3.4.

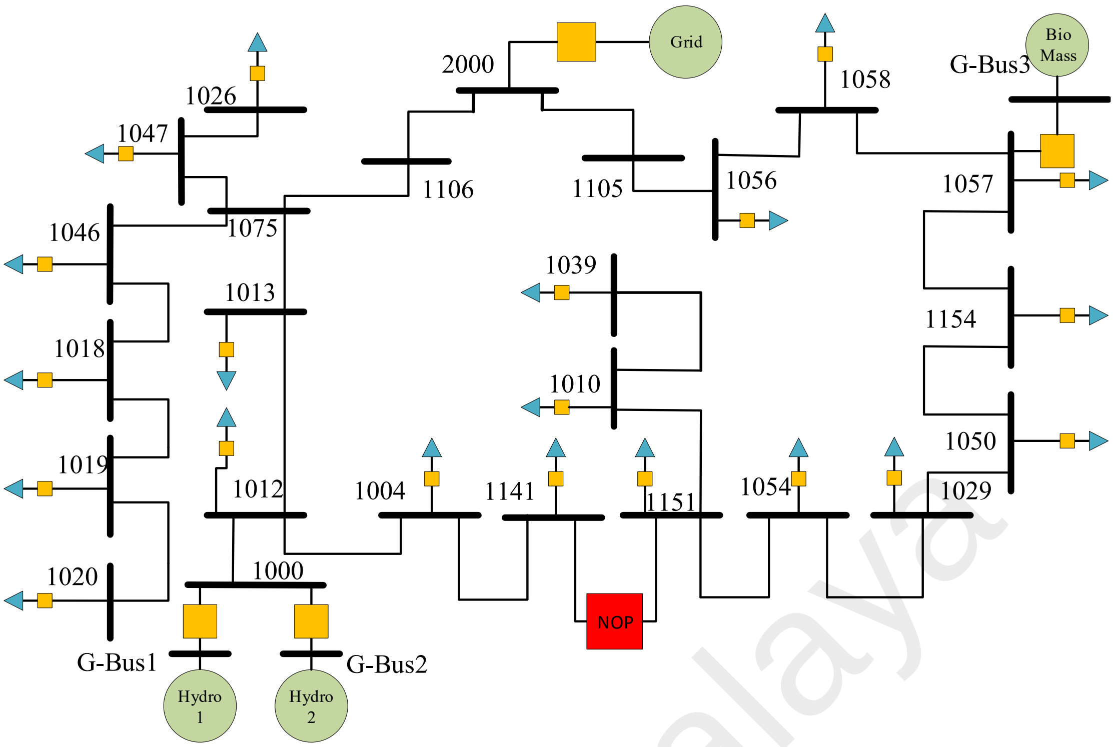

Figure 3.4: 11kV-28 bus Malaysian distribution system.

The distribution network and transmission grid are interconnected through a grid circuit breaker (*BRKG*). A step-down transformer unit (132 kV/11 kV, 50 MVA) is used to stepdown the transmission grid supply. The exciter, governor, and turbine for a DG are modeled with standard models available in the PSCAD library. All the parameters are set to default values given in PSCAD library for exciter, PID controller, Turbine, and governor models. A snapshot of the modeled test system in PSCAD is presented in Figure 3.5.

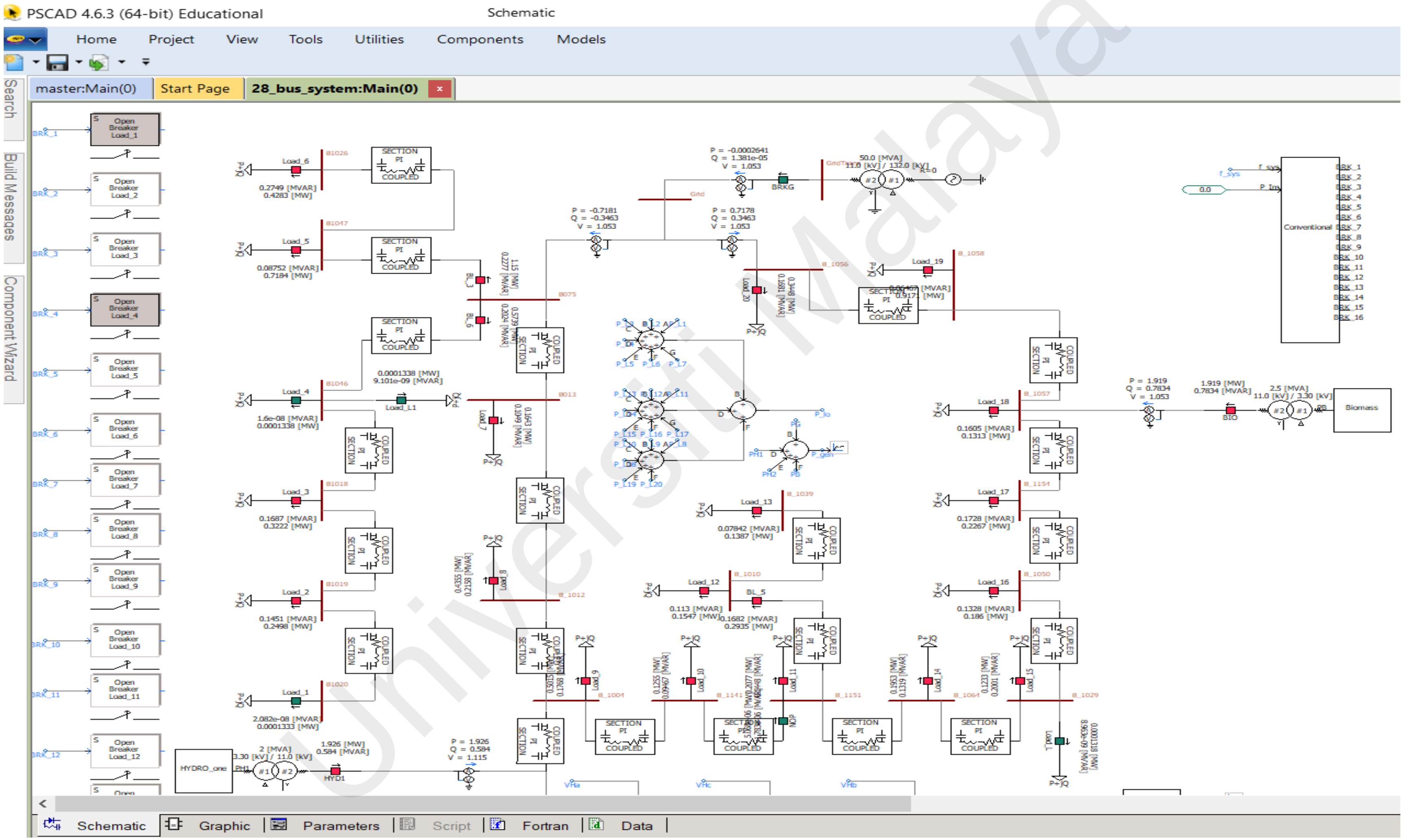

Figure 3.5: PSCAD modeling of 11kV-28 bus Malaysian distribution system.

Classification of loads as non-critical, semi-critical, or critical is based on the type of load, i.e., residential, industrial, municipal, and commercial. Loads ranked 1 to 11 are assumed to be residential loads therefore prioritized as non-critical, loads ranked 12 to 16 are supposed to be commercial load thus classified as semi-critical, and the remaining four loads are assumed to be very important, hence given the critical priority, as in Table 3.1.

Table 3.1: Load data for 11kV-28 bus system.

Priority	Load ranking	Bus No.	Load	
			P (MW)	**Q (MVAR)**
Non-critical	1	1050	0.044	0.04
	2	1013	0.069	0.042
	3	1047	0.059	0.088
	4	1026	0.091	0.028
	5	1012	0.314	0.125
	6	1010	0.45	0.08
	7	1039	0.4532	0.244
	8	1020	0.078	0.06
	9	1019	0.22	0.14
	10	1018	0.2	0.12
	11	1046	0.32	0.16
Semi-critical	12	1141	0.22	0.214
	13	1064	0.22	0.192
	14	1057	0.46	0.125
	15	1058	0.385	0.213
	16	1154	0.315	0.126
Critical	17	1004	0.33	0.128
	18	1151	0.455	0.106
	19	1056	0.595	0.344
	20	1029	0.532	0.425

3.6.2 IEEE 69 bus distribution System

The IEEE 69-bus system load data were taken from (Muhammad et al., 2019) and presented in Table 3.3; one bio-mass DG and two hydro DGs were placed in an optimal location with optimal ratings, as proposed in (Muhammad et al., 2019) and shown in Table 3.2. A single line diagram of the system is shown in Figure 3.6. This system consists of 48 lumped loads and three DGs: two mini-hydro DGs and one bio-mass DG. The DGs and loads for this system were modeled with the standard components available in the PSCAD library. The loads were prioritized as critical, semi-critical, and non-critical. Loads ranked 1 to 24 were assumed to be non-critical, loads ranked 25 to 36 were classified as semi-critical, and the remaining 12 loads were categorized as critical.

Table 3.2: Optimal DG size and location (Muhammad et al., 2019).

DG	Bus No.	P (MW)	Q (MVAR)
Hydro 1	11	0.79	0.54
Hydro 2	49	0.86	0.62
Biomass	61	1.59	1.13

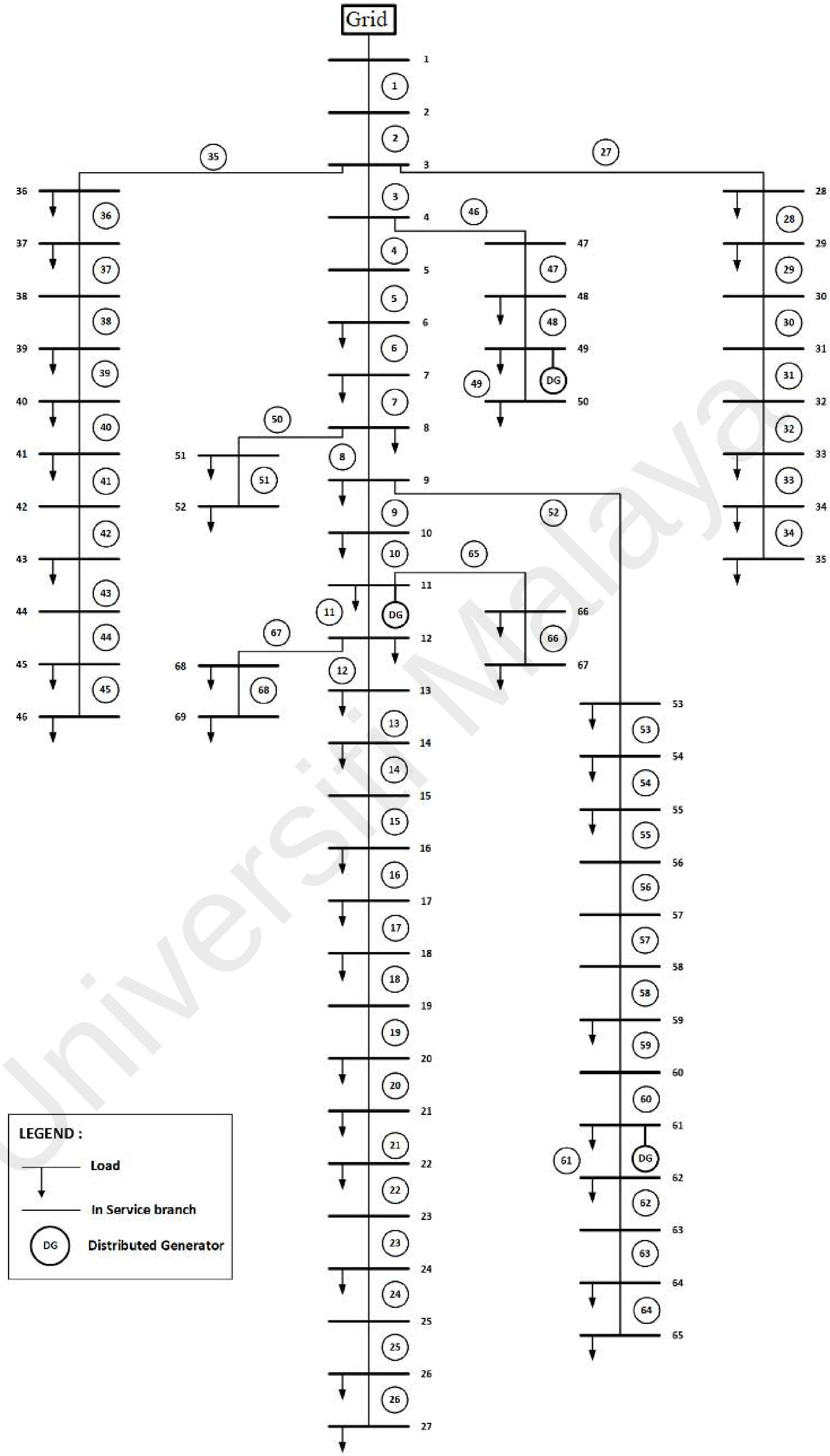

Figure 3.6: IEEE 69 bus distribution system.

Table 3.3: IEEE 69 bus system data (Savier & Das, 2007).

Branch	From	To	R (ohms)	X (ohms)	Length Km
1	1	2	0.0005	0.0012	**0.7**
2	2	3	0.0005	0.0012	**0.65**
3	3	4	0.0015	0.0036	**0.77**
4	4	5	0.0251	0.0294	**0.77**
5	5	6	0.3660	0.1864	**0.77**
6	6	7	0.3811	0.1941	**0.68**
7	7	8	0.0922	0.0470	**0.78**
8	8	9	0.0493	0.0251	**0.78**
9	9	10	0.8190	0.2707	**0.76**
10	10	11	0.1872	0.0619	**0.7**
11	11	12	0.7114	0.2351	**0.71**
12	12	13	1.0300	0.3400	**0.69**
13	13	14	1.0440	0.3450	**0.75**
14	14	15	1.0580	0.3496	**0.76**
15	15	16	0.1966	0.0650	**0.67**
16	16	17	0.3744	0.1238	**0.74**
17	17	18	0.0047	0.0016	**0.67**
18	18	19	0.3276	0.1083	**0.71**
19	19	20	0.2106	0.0690	**0.7**
20	20	21	0.3416	0.1129	**0.66**
21	21	22	0.0140	0.0046	**0.73**
22	22	23	0.1591	0.0526	**0.7**
23	23	24	0.3463	0.1145	**0.73**
24	24	25	0.7488	0.2475	**0.76**
25	25	26	0.3089	0.1021	**0.68**
26	26	27	0.1732	0.0572	**0.66**
27	3	28	0.0044	0.0108	**0.7**
28	28	29	0.0640	0.1565	**0.69**
29	29	30	0.3978	0.1315	**0.78**
30	30	31	0.0702	0.0232	**0.74**
31	31	32	0.3510	0.1160	**0.77**
32	32	33	0.8390	0.2816	**0.78**
33	33	34	1.7080	0.5646	**0.79**
34	34	35	1.4740	0.4873	**0.73**

Table 3.3 continued

Branch	From	To	R (ohms)	X (ohms)	Length Km
35	3	36	0.0044	0.0108	**0.68**
36	36	37	0.0640	0.1565	**0.72**
37	37	38	0.1053	0.1230	**0.71**
38	38	39	0.0304	0.0355	**0.79**
39	39	40	0.0018	0.0021	**0.72**
40	40	41	0.7283	0.8509	**0.71**
41	41	42	0.3100	0.3623	**0.71**
42	42	43	0.0410	0.0478	**0.66**
43	43	44	0.0092	0.0116	**0.71**
44	44	45	0.1089	0.1373	**0.78**
45	45	46	0.0009	0.0012	**0.78**
46	4	47	0.0034	0.0084	**0.74**
47	47	48	0.0851	0.2083	**0.77**
48	48	49	0.2898	0.7091	**0.74**
49	49	50	0.0822	0.2011	**0.79**
50	8	51	0.0928	0.0473	**0.73**
51	51	52	0.3319	0.1114	**0.65**
52	9	53	0.1740	0.0886	**0.77**
53	53	54	0.2030	0.1034	**0.75**
54	54	55	0.2842	0.1447	**0.78**
55	55	56	0.2813	0.1433	**0.71**
56	56	57	1.5900	0.5337	**0.7**
57	57	58	0.7837	0.2630	**0.7**
58	58	59	0.3042	0.1006	**0.69**
59	59	60	0.3861	0.1172	**0.75**
60	60	61	0.5075	0.2585	**0.79**
61	61	62	0.0974	0.0496	**0.79**
62	62	63	0.1450	0.0738	**0.71**
63	63	64	0.7105	0.3619	**0.75**
64	64	65	1.0410	0.5302	**0.66**
65	11	66	0.2012	0.0611	**0.65**
66	66	67	0.0047	0.0014	**0.76**
67	12	68	0.7394	0.2444	**0.69**
68	68	69	0.0047	0.0016	**0.77**

3.6.3 IEEE 137 bus distribution System

The IEEE 137 bus system is made up of two IEEE 69 bus systems connected in parallel with the same grid to form a 137 bus system. This system is comprised of six DGs, *i.e.,* four hydro DGs and two biomass DGs. The load data is same as presented for the IEEE 69 bus system above. Load ranking is also utilized with same priority, as is explained for the IEEE 69 bus system. A block diagram of this system is shown in Figure 3.7.

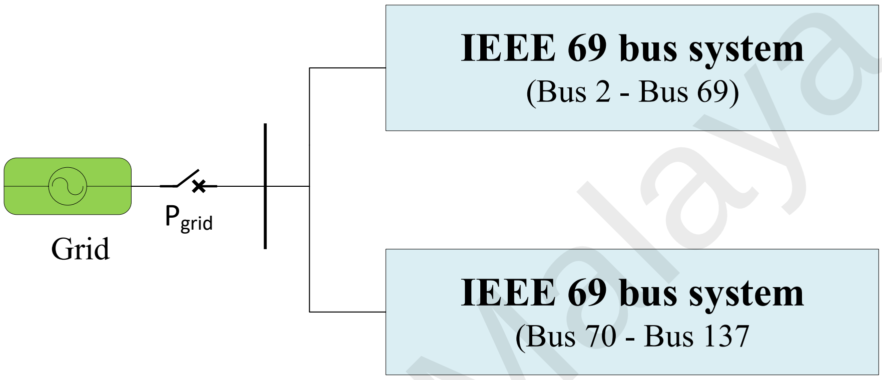

Figure 3.7: IEEE 137 bus system.

3.6.4 Modeling of system equipment

All three systems were modeled in PSCAD. The IEEE type AC1A exciter was used to model the synchronous generator. The hydro DG governor was modeled with a PID controller, and the hydraulic turbine was modeled using non-elastic water columns without a surge tank, which is available in the PSCAD master library. The biomass DG was modeled using a mechanical, hydraulic governor with PID control and a generic turbine model, which included the intercept valve effect. A schematic view of biomass DG modeled in PSCAD is shown in Figure 3.8.

DGs generate electrical power at a terminal voltage of 3.3kV for the test systems used in this research. Therefore, the transformer is required to step up the voltage to 11kV to supply local loads in the distribution system. Moreover, grid supply also needs to be stepped down from 132kV to 11kV using a step-down transformer. A basic two winding transformer model available in the PSCAD library is used in this research in delta star configuration.

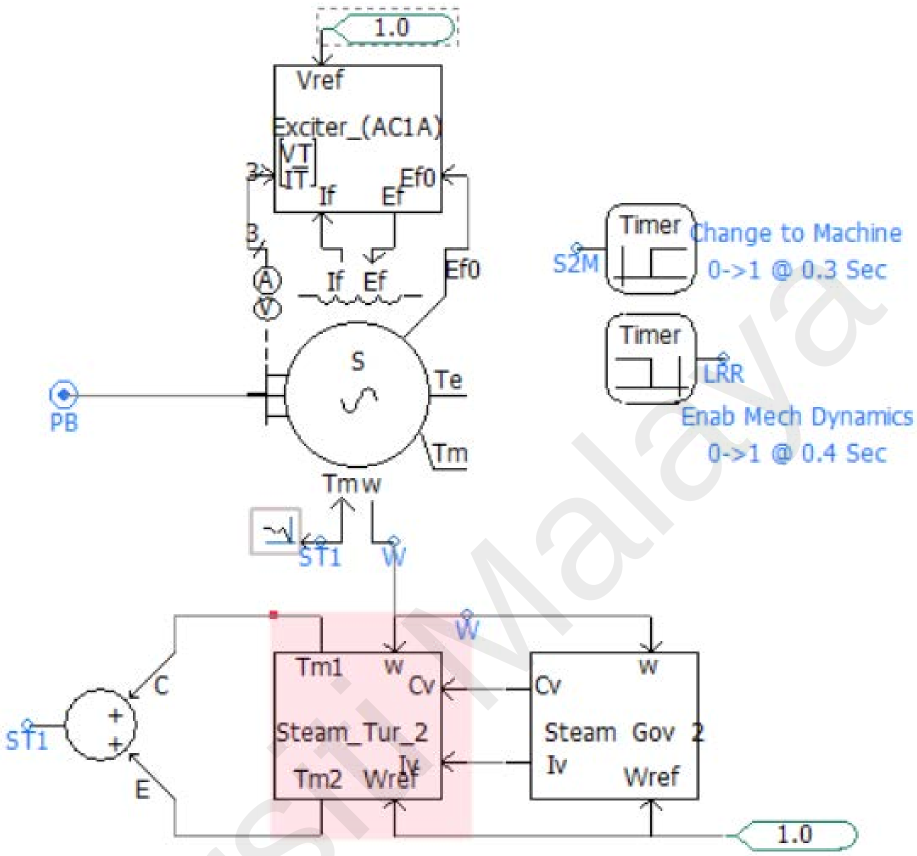

Figure 3.8: Synchronous generator model in PSCAD.

Loads were modeled as voltage- and frequency-dependent loads using the standard load model in the PSCAD library. Loads are modeled in this research as voltage and frequency-dependent static loads. A fixed load model available in the PSCAD library is used in this research. The active and reactive power of load for this model is calculated in terms of following mathematical relations.

$$P = P_o.\left(\frac{V}{V_o}\right)^{NP}.(1 + K_{PF}.dF) \quad (3.13)$$

$$Q = Q_o.\left(\frac{V}{V_o}\right)^{NQ}.(1 + K_{QF}.dF) \quad (3.14)$$

Where P is equivalent load real power, P_o rated real power per phase, V is load voltage, V_o is rated load voltage (RMS, L-G), NP is dP/dV voltage index for real power, K_{PF} is dP/dF frequency index for real power, Q is equivalent load reactive power, Q_o is rate reactive power (+inductive) per phase, NQ is dQ/dV voltage index for reactive power, and K_{QF} is dQ/dF frequency index for reactive power.

The proposed PIFM and ILSM modules are designed as a new PSCAD component with multiple inputs and outputs. Its script is coded in FORTRAN compiler to call the MATLAB function. FORTRAN compiler communicates between PSCAD and MATLAB during real-time simulation and calls the MATLAB function to actuate the load shedding scheme when the frequency and its rate of change approaches beyond a threshold value.

3.6.5 Modeling of Conventional UFLS

The modeling of the conventional technique in this research is based on eight-step load shedding scheme proposed in (Laghari et al., 2015). UFLS relay settings are based on a fixed amount of predefined load, sequentially disconnected for each drop of 0.2Hz in the system frequency, starting from 49.5Hz. If the frequency is not stabilized in the first four steps, then the next four steps are activated for each drop of 0.1Hz in the system frequency until the system frequency starts to recover towards stability. The detailed predefined load shedding relay settings are presented in Table 3.4. It has been verified that the eight-step conventional load shedding scheme attains better results in comparison to 4, 6, and 10 steps. It can be seen from Figure 3.9 below that the eight-step load shedding technique produces the best results with lesser overshoot.

Table 3.4: Relay settings for conventional technique

Step	Loads	Threshold	Step	Loads	Threshold
1	1,2,3	49.5	5	10,11	48.8
2	4,5	49.3	6	12	48.7
3	6,7	49.1	7	13,14	48.6
4	8,9	48.9	8	15,16	48.5

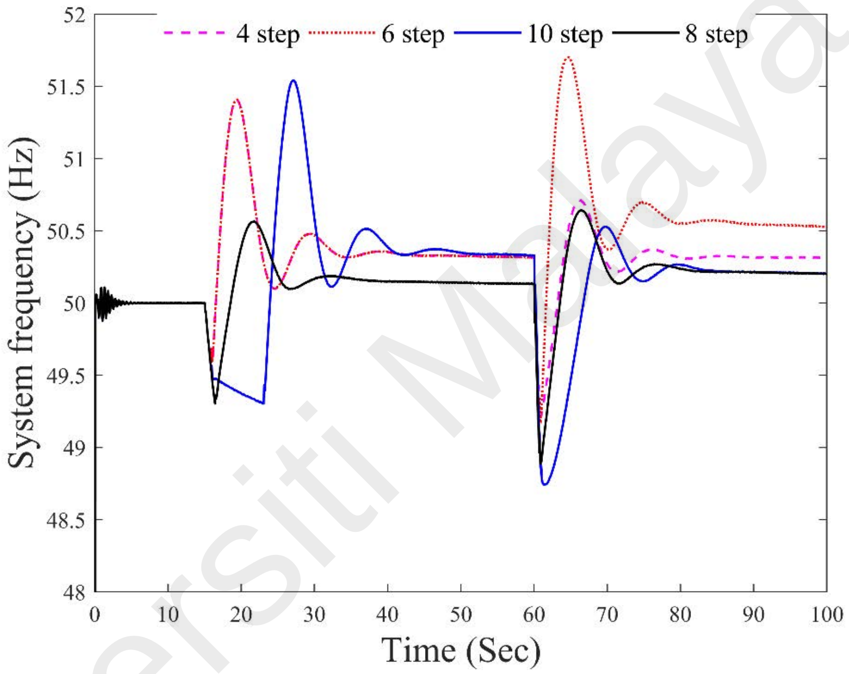

Figure 3.9: Comparison of SFR for multistep conventional load shedding.

3.6.6 Modeling of UFLS Adaptive Techniques

For adaptive-I technique, the method in (Laghari et al., 2015) is simulated. The power imbalance was estimated using the swing equation, and the exhaustive search technique is applied to find the combination of loads for shedding. A MATLAB function is coded that accepts the power imbalance and real-time load values as input. This function will perform an exhaustive search to optimize the best possible combination from selected loads and return the circuit breaker status in binary as output for all loads. A new block is designed in PSCAD that is able to communicate in real-time simulation between

MATLAB and PSCAD. The designed block in PSCAD receives the circuit breaker status from MATLAB and transmits a trip signal to selected circuit breakers for operation.

Adaptive-II technique is also modeled by creating a new PSCAD block that communicates with MATLAB function. A MATLAB function is programmed to calculate the stability index of all load busses and arrange them in ascending order according to their load priority. These ordered loads are shed sequentially to balance the power mismatch estimated from the PIFM module.

To consider practical aspects in the simulation, circuit breaker operation time, and communication delay between grid operation and load center, is assumed 100ms as in (Anderson & Mirheydar, 1992). Furthermore, the remote circuit breaker operation facility and the real-time measurements were assumed to be available for all the connected loads. In this simulation, a Core i5, 9th generation pc was used for the simulation with a step time of 270uS on PSCAD (4.5.3) professional version interfaced with MATLAB R2014b.

3.7 Summary

The analysis of existing load shedding techniques manifests that each load shedding scheme is composed of two modules, i.e., power mismatch calculation module and selection of load module. This chapter explains the detailed methodology for both modules of load shedding proposed in this research. Power imbalance forecasting modules utilize a basic machine learning algorithm called polynomial regression to forecast the power imbalance in the system for any contingency. The intelligent load shedding module optimizes the load shedding by disconnecting the non-critical loads to endorse the functionality of critical loads. Furthermore, the voltage stability index of loads is also used to prioritize the loads for selection in the proposed load shedding module to avoid operation of voltage protection at relatively unstable buses. The test systems used for validation of proposed research are also explained in this chapter.

Modeling of different power system components from the PSCAD library is also explained.

CHAPTER 4: RESULTS AND DISCUSSIONS

4.1 Introduction

The effectiveness of the proposed UFLS scheme has been analyzed by comparing the results with conventional and two adaptive load shedding schemes. Various contingencies, *i.e.,* intentional islanding, overloading, DG tripping, and cascaded outage of DGs, were simulated for the test systems to observe the behavior of load shedding schemes. Four different scenarios have been investigated incorporating three test systems, *i.e.,* Malaysia 28-bus system, the IEEE 69-bus system, and the IEEE 137-bus system. Furthermore, the effectiveness of the proposed power imbalance forecasting module has also been investigated, and the results were compared with conventional and adaptive techniques.

4.2 Development of power imbalance equation

The first step is to develop the Power Imbalance equation. This is done by simulating different loading conditions and contingencies. A graphical presentation of different polynomials fitting the data is shown in Figure 4.1. Table 4.1 showed the comparison for the goodness of fit for all the polynomials. From this analysis, it can be observed that the quintic polynomial best suits the given system data, as it presents the minimum RMSE value and better fits the R_square percentage.

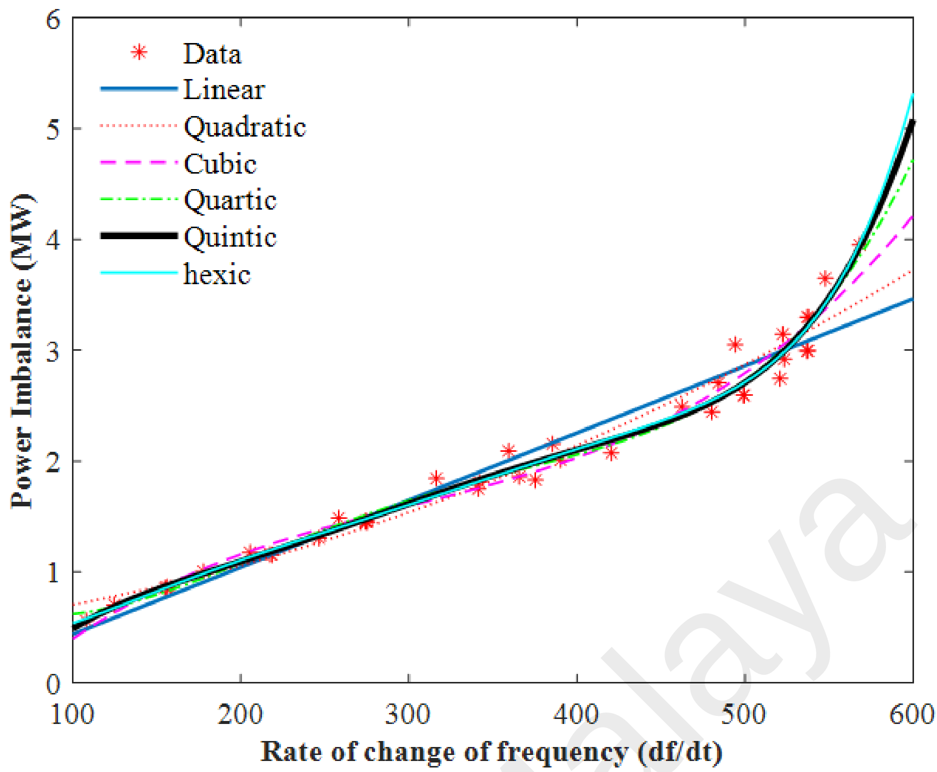

Figure 4.1: Polynomial Regression for Power Imbalance.

Table 4.1: Comparison Table for the Goodness of Fit

Parameters	**Linear**	**Quadratic**	**Cubic**	**Quartic**	**Quintic**	**Hexic**
SSE	1.5716	1.1698	0.7753	0.6298	**0.5942**	0.5865
R-Square	0.947	0.9606	0.9739	0.9788	**0.9803**	0.9802
DFE	37	36	35	34	**33**	32
ADJR-Square	0.9456	0.9584	0.9716	0.9763	**0.9769**	0.9765
RMSE	0.2061	0.1803	0.1488	0.1361	**0.1342**	0.1354

Where SSE in the table stands for sum of squared estimate of errors, DFE stands for degree of freedom for error and RMSE stands for room mean square error. Whereas R-Square is the measure of how close the data fits with the regression line. The system frequency response is analyzed for all the polynomials used in the PIFM module to verify that the quintic polynomial is the most suitable one to forecast the power imbalance based on rate of change of frequency. The result of the contingency simulation is shown in Figure 4.2.

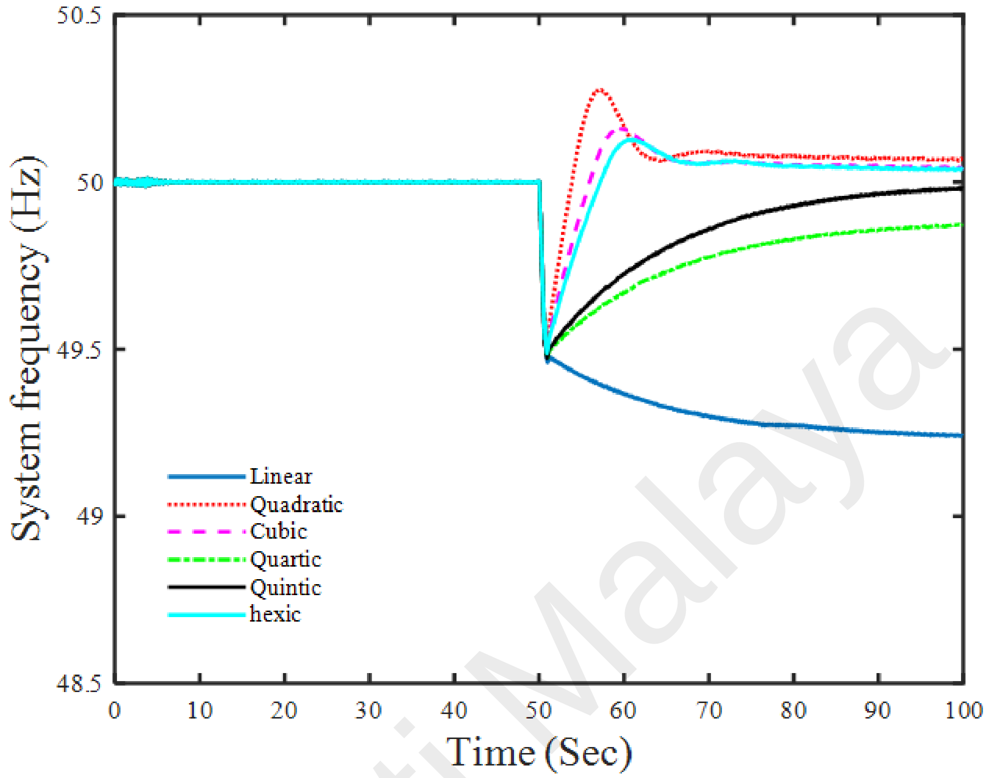

Figure 4.2: Frequency Response for Different Polynomial PI Predictions.

It is evident that the quintic (5^{th}-degree) polynomial can accurately forecast power mismatches and that the frequency is smoothly stabilized for forecasting without any overshoots. Therefore, the quintic polynomial was used for the proposed load shedding scheme to forecast the power imbalance. Three different scenarios (shown in Table 4.2 were simulated in this research for comparison to prove the robustness and superiority of the proposed technique. The scenarios are arranged in an unsymmetrical way to validate the different objectives. 28 bus system is simulated in each scenario as a base test system. Whereas, IEEE 137 bus system and IEEE 69 bus system are simulated in scenario-I and Scenario-II to justify the efficacy of the proposed scheme. The basic objective is to testify the performance of the proposed load shedding with increasing number of loads for a large-scale test system.

Table 4.2: Case studies for validation of proposed technique.

Scenarios	Events	Test System	SFR Comparison	Objective
Scenario-I	• Islanding • DG tripping • Blackout	28-bus system	• Proposed technique with load priority only • Adaptive-I technique • Conventional	• Validate the proposed PIFM module performance • Validate the effect of increasing number of loads on the proposed ILSM module
	• Islanding • DG tripping	IEEE 137 bus system	• Proposed technique with load priority only	
Scenario-II	• Islanding • DG tripping • Overloading	28-bus system	• Proposed technique with load priority and stability index • Adaptive-I technique • Adaptive-II technique • Conventional	• Validate the performance of proposed MILP model to find optimal load combination based on different load priorities
	• Islanding • DG tripping	IEEE 69 bus system		
Scenario-III	• Islanding • DG tripping	28-bus system	• Proposed technique without priority • Proposed technique with load priority only • Proposed technique with load priority and stability index both	• Validate the importance of voltage stability index for UFLS techniques

4.3 Scenario I

The objective function of the proposed mathematical model, to optimize the load shedding in this scenario, is shown in Equation 4.1. The proposed objective function is simplified to validate that the proposed intelligent load shedding module finds the optimal combination of loads as accurate as by exhaustive search in (Laghari et al., 2015).

$$OF = \min\left[\sum_{j\in NCL}\alpha.x_j + \sum_{k\in SCL}\beta.x_k + \sum_{l\in CL}\gamma.x_l + \delta.w\right] \tag{4.1}$$

Where *α, β* and *γ* are proposed priority of loads, *x* is the binary variable that shows the status of circuit breaker; *0* for disconnected and *1* for connected, *w* is the dummy variable for MILP optimization to satisfy the constraints and δ is its coefficient.

4.3.1 Test results for 28 bus system (Scenario-I)

Three different contingencies, *i.e.,* intentional islanding, DG tripping, and cascaded outage of DGs, were carried out on the 28-bus system to validate the performance of the proposed power imbalance forecasting module. The details of the system have been presented in Section 3.6.1 and Figure 3.4. The loads were prioritized as critical, semi-critical, and non-critical based on their types. The load priority utilized for proposed and adaptive techniques is shown in Table 4.3 and the test system data is presented in

Table 4.4.

Table 4.3: Load Priority Table for the Proposed and Adaptive Techniques.

Adaptive	Random		Fixed
Load rank	1-16		17-20
Proposed	Critical	Semi-critical	Non-critical
Load rank	17-20	12-16	1-11

Table 4.4: Load data for the Malaysian distribution system.

Load Rank	**Bus No.**	**P (MW)**	**Q (MVAR)**	**Load Rank**	**Bus No.**	**P (MW)**	**Q (MVAR)**
1	1020	0.078	0.060	11	1151	0.453	0.244
2	1019	0.221	0.140	12	1010	0.451	0.192
3	1018	0.211	0.126	13	1039	0.455	0.426
4	1046	0.321	0.088	14	1054	0.221	0.040
5	1047	0.059	0.028	15	1029	0.534	0.126
6	1026	0.091	0.042	16	1050	0.044	0.125
7	1013	0.069	0.125	17	1154	0.316	0.213
8	1012	0.315	0.128	18	1057	0.451	0.345
9	1004	0.331	0.106	19	1058	0.386	0.344
10	1141	0.221	0.080	20	1056	0.597	0.425

4.3.1.1 Islanding Event (Scenario-I)

An intentional islanding event was simulated at time t =15 s by disconnecting the grid coupling circuit breaker (BRKG). In this scenario, the total generation capacity of the system was 5.50 MW at the rated conditions, which was less than the total load demand of 5.86 MW on the island. The difference between the load demand and the generated power caused a power imbalance in the system, resulting in a decline in the frequency. The proposed scheme analyzed this decline in frequency and forecasted a power imbalance of 0.358 MW in the system. This imbalance was more than threshold value set for this technique, which was 0.05 MW. Hence this power imbalance value was transmitted to the ILSM module. The ILSM module computed the load combination to be shed for the power imbalance while considering the load priorities. Then, it transmitted the trip signal to the breakers to shed the selected loads. The detailed load shedding parameters for the proposed, adaptive, and conventional techniques are shown in Table 4.5. The frequency response of this test is presented in Figure 4.3.

Table 4.5: Frequency Stability Parameters for Islanding event (Scenario-I).

Parameters	Conventional	Adaptive	Proposed
Power mismatch (MW)	0.358	0.36	0.358
Load shed amount (MW)	0.51	0.361	0.358
Loads disconnected	1,2,3	8,16	1,5,10
Undershoot (Hz)	49.3	49.46	49.46
Overshoot (Hz)	50.56	50.03	-
Extra load shed (MW)	0.152	0.001	0
Total connected load	5.32	5.483	5.488

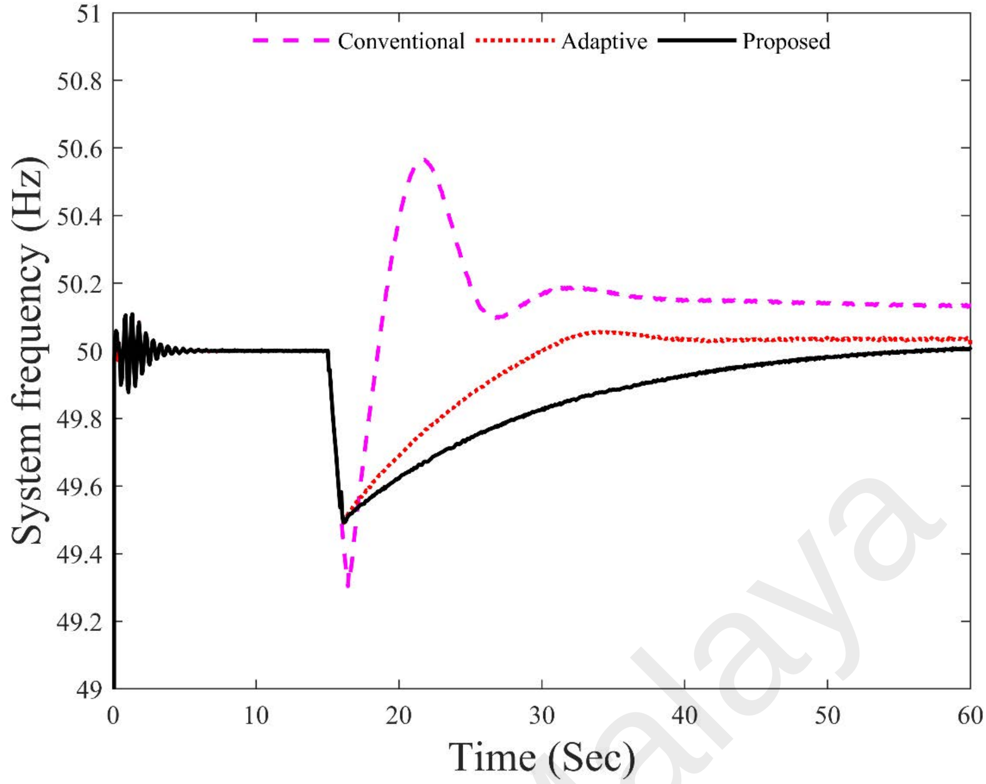

Figure 4.3: Frequency Response for Islanding (Scenario-I).

It is visible from Figure 4.3 that there was a high overshoot of 50.56Hz due to the excessive load shedding in the case of the conventional technique, as the excessive load shedding resulted in a prompt increase in the frequency and caused overshoot. Figure 4.3 also shows a comparison of power imbalance measured using swing equation and proposed PIFM module. Power imbalance measured using swing equation for adaptive technique produced a slight overshoot in frequency response as compared to frequency response for the proposed technique.

The adaptive technique based on the exhaustive search and swing equation also exhibited an overshoot of 50.03 Hz in comparison with the proposed research due to an error in the power mismatch calculation. The power imbalance estimated for the adaptive scheme was 0.36 MW. Therefore, an extra load was shed, which caused this overshoot. Moreover, the load 16 was selected in addition to load 8, which is prioritized as semi-critical load. However, the frequency response in Figure 4.3 proves that the proposed technique accurately predicted the power imbalance as 0.358MW and that the non-critical loads 1, 5, and 10 were selected to be shed. Moreover, Figure 4.3 and Table 4.5 show that the load retained in the system after the event was high for the proposed technique.

4.3.1.2 DG tripping in islanded system (Scenario-I)

A distribution system operating in islanding is vulnerable to instability due to unplanned disconnection of a DG, which may yield a cascaded blackout. Hence a load shedding scheme should be able to compensate this condition to prevent the system from a blackout. In this case, the largest DG capacity, which is biomass DG was disconnected from the system at time t = 60 s when the system was at the steady-state condition after islanding. After the load shedding, the connected loads to the system were 5.488 MW, 5.483 MW, and 5.32 MW for the proposed, adaptive and conventional techniques, respectively. The detailed load shedding parameters are presented in Table 4.6. Figure 4.4 shows the frequency response of the system.

Table 4.6: Frequency Stability Parameters for DG Tripping (Scenario-I).

Parameters	Conv.	Adap.	Prop.
Power mismatch (MW)	1.878	1.881	1.878
Load shed amount (MW)	1.868	1.882	1.874
Loads disconnected	1-11	5-11,13, 14,16	1,2,3, 5-10,15
Undershoot (Hz)	48.6	48.87	48.97
Overshoot (Hz)	50.62	50.15	-
Extra load shed (MW)	-0.01	0.001	-0.004
Total connected load	3.46	3.578	3.602

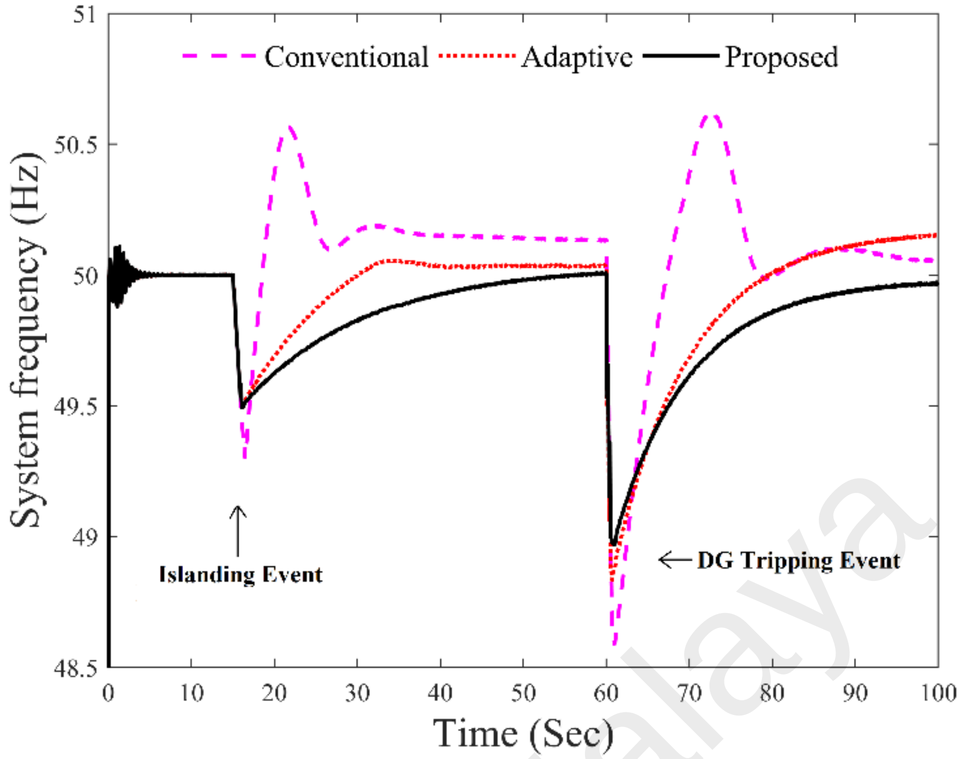

Figure 4.4: Frequency Response for DG Tripping (Scenario-I).

The proposed scheme sheds the non-critical loads 2, 3, 6, 7, 8, 9, and one semi-critical load 15 in addition to the previously selected loads in case (1) for a predicted power imbalance of 1.878 MW. It can be observed from Figure 4.4 that the frequency was stabled for the proposed technique without any overshoot, making it optimal in comparison with the overshoot of 50.15Hz and 50.62Hz that took place with the adaptive and conventional techniques, respectively. The overshoot in the adaptive technique was due to an error in estimating the power imbalance in the system. Moreover, the loads 13, 14, and 16 were selected to be shed in the case of the adaptive technique, which is prioritized as semi-critical loads. The analysis of the load shedding parameters in Table 4.6 and Figure 4.5 depicts that the load retained in the system for the proposed technique was 3.602 MW, which is higher than in the other schemes.

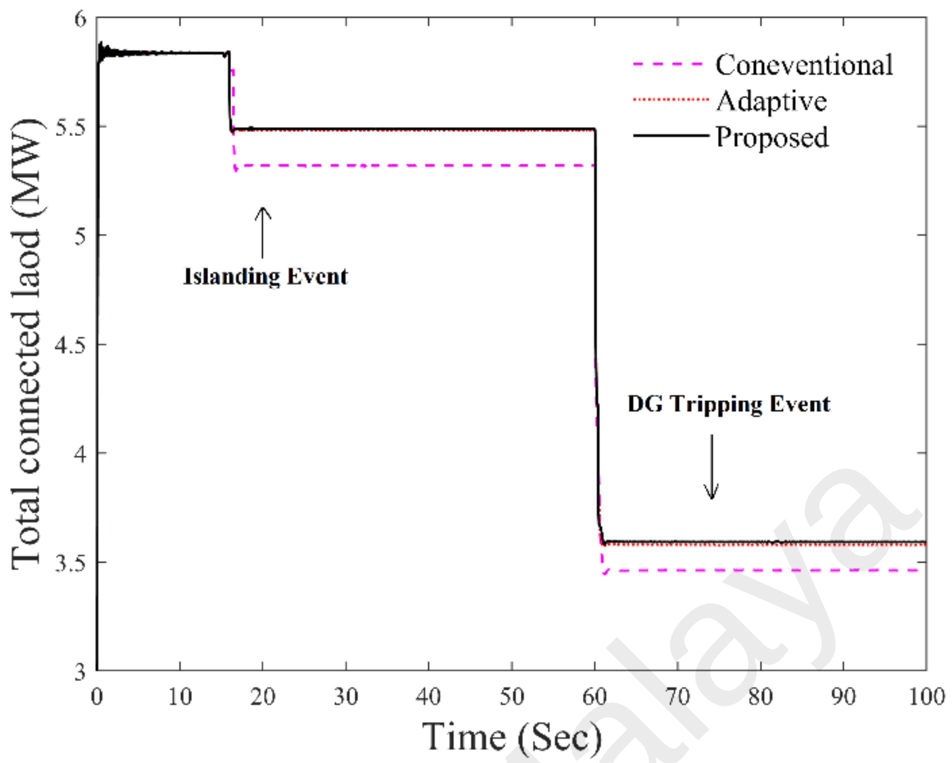

Figure 4.5: Real-Time Total Load of the 28 Bus System (Scenario-I).

4.3.1.3 Cascaded DG tripping in islanded system (Scenario-I)

An islanded system is vulnerable to cascaded tripping of DGs due to unstable parameters. A load shedding technique should be able to avoid blackouts in such a case. Therefore, cascaded tripping of two out of three DGs in the islanded system was simulated at time t = 60 s to observe the response of the proposed technique. The detailed load shedding parameters are listed in Table 4.7and Figure 4.6 shows the frequency response for this scenario.

It can be observed from Figure 4.6 that the proposed technique estimated the power imbalance as 3.612 MW, and all non-critical and semi-critical loads are disconnected except load 7 and 16. The frequency was restored to almost nominal value with ensured supply is available to critical loads. Frequency response for conventional technique is unstable and fluctuating, suggesting that excessive load shedding has been performed. On the other hand, adaptive technique finds a combination of loads that results in inadequate load shedding.

Table 4.7: Frequency Stability Parameters for cascaded DG tripping.

Parameters	Conventional	Adaptive	Proposed
Power mismatch (MW)	3.612	3.605	3.61
Load shed amount (MW)	3.62	3.588	3.607
Loads disconnected	1-15	1-4,6,8-16	1-6,8-15
Undershoot (Hz)	48.42	48.74	48.85
Overshoot (Hz)	50.97	-	-
Excessive load shed (MW)	0.08	-0.017	-0.003
Total connected load	1.82	1.88	1.85

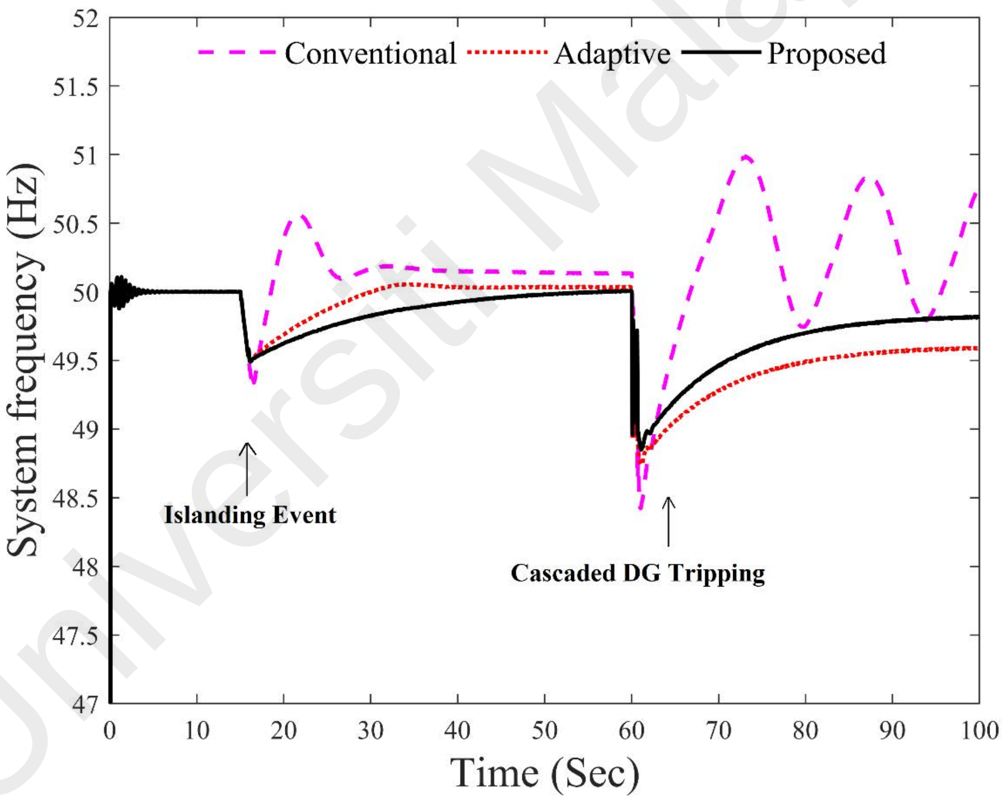

Figure 4.6: Frequency response for cascaded DG tripping.

4.4 Test results for IEEE 137 bus system

The IEEE 137 bus system contains 96 lumped loads. The load data for IEEE 69 bus system is used with the same load priority to test the efficacy of the proposed technique for a large-scale system. Islanding and DG tripping events were simulated to observe the frequency response for this system. The frequency response is shown in Figure 4.7, and detailed load shedding parameters for the said events are presented in Table 4.8.

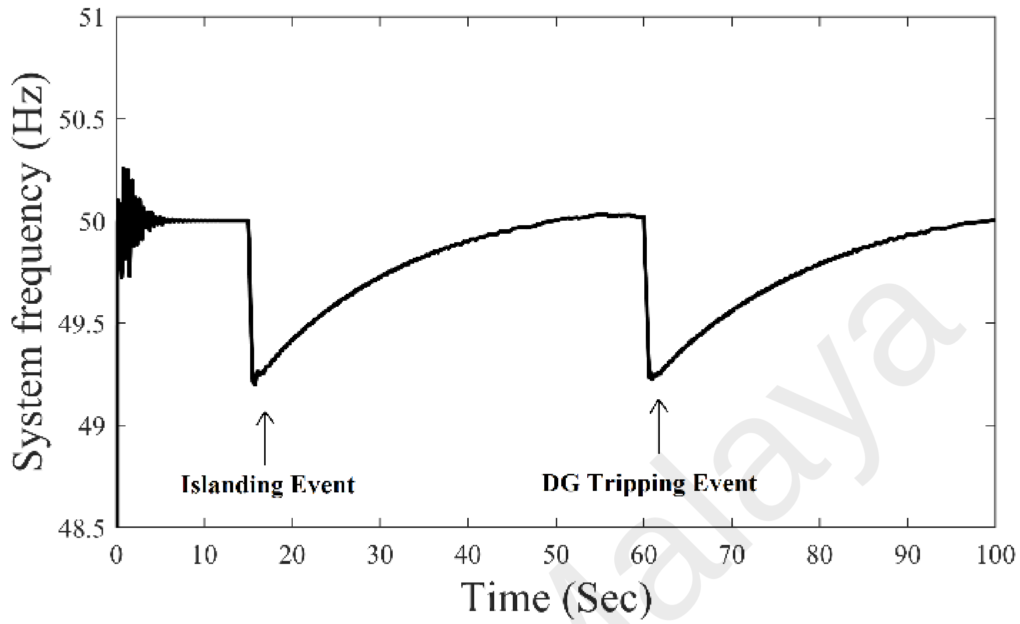

Figure 4.7: Frequency response for IEEE 137 bus system.

It can be observed from Figure 4.7 that the proposed scheme performs accurate load shedding for both islanding and DG's tripping events. Frequency is stabilized to nominal value without any overshoot. Moreover, Table 4.8 indicates that only non-critical loads were shed for the islanding event for a power imbalance of 1.102 MW. Whereas, when a DG is disconnected from the system in islanding operational state, the power imbalance is greater than total non-critical loads in the system. Hence, two semi-critical loads in addition to most of the non-critical loads have been shed to perform optimal load shedding incorporating load priority.

Table 4.8: Load shedding parameters for IEEE 137 bus system.

Parameters	Islanding	DG tripping
Power Imbalance (MW)	1.102	0.895
Extra load shed (MW)	0	0
Loads disconnected	3,6,7,14,16,39,41, 42,43,48,50,52	1-12,14,16-22,24,32, 37-50,52-58,60,68
Frequency Undershoot (Hz)	49.16	49.22
Frequency overshoot (Hz)	50.02	-

The inspection of the simulation results in this scenario shows that accurate power imbalance forecasting and finding a combination of loads are two different problems and that an optimal solution is needed for both of them. Although the adaptive-I technique based on an exhaustive search tool generates accurate results, the storage space required to evaluate and store the 2^n combinations is infeasible when the number of loads is above a specific limit. Therefore, an increase in the number of loads makes the adaptive-I technique infeasible for large systems, *i.e.,* IEEE 69 bus system and IEEE 137 bus system. The possible combinations for IEEE 137 bus systems reach $7.92*10^{28}$. It becomes highly impossible to evaluate these combinations making the adaptive technique infeasible and unreal. However, the proposed scheme performs optimal load shedding, irrespective of increase in number of loads, and sheds mostly non-critical loads based on given priorities. Therefore, the proposed mixed-integer linear programming optimization efficiently solves the same problem. On the other hand, the proposed PIFM module forecasted a more accurate power imbalance for severe contingencies as compared to adaptive-I technique. The accurate power imbalance estimation, along with optimal load shedding selection, makes the proposed technique a better solution.

4.5 Scenario II

In this scenario, the proposed technique based on load priority and stability index was compared with the conventional and both adaptive techniques to validate the efficacy. The proposed scheme used the objective function that incorporates load priority based on voltage stability index and type of load. The objective function is shown in Equation (4.2).

$$OF = \min \sum_{j \in NCL} \alpha.SI_j.x_j + \sum_{k \in SCL} \beta.SI_k.x_k + \sum_{l \in CL} \gamma.SI_l.x_l + \delta.w \tag{4.2}$$

Where *α, β* and *γ* are proposed priority of loads, *x* is the binary variable that shows the status of circuit breaker; 0 for disconnected and 1 for connected , *SI* is the stability index of load busses, *w* is the dummy variable for MILP optimization to satisfy the constraints and δ is its coefficient.

4.5.1 Test results for the 28-bus system (Scenario-II)

The details of the system have been presented in Section 3.6.1, Figure 3.4, and Table 3.1. Thirteen loads from the 28 bus system were selected to form eight load groups (shown in Table 4.9) and were used for load shedding in the adaptive-I technique presented in (Laghari et al., 2015). The adaptive-I technique was also simulated in this scenario with all the system loads to test the effect of increasing the number of loads on the methodology (Laghari et al., 2015).

The results of another adaptive technique based on the stability index of loads (Adaptive-II) were also compared in this scenario. The Adaptive-II technique calculated the stability index of each load bus when there was a power imbalance in the system, and loads were sequentially detached based on their stability index until the load shed amount was equal to or higher than the power imbalance. For each event, the power mismatch calculation module determined the power imbalance, and subsequently handed over the estimated power mismatch value to the load shedding module and activated the stability index module for the proposed technique.

Table 4.9: Load data for the adaptive technique.

Loads Ranked	Bus No.	P (MW)
'a' (1)	1050	0.044
'b' (2)	1013	0.069
'c' (3,4)	1047,1026	0.15
'd' (5)	1012	0.314
'e' (6,7)	1010,1039	0.903
'f' (8-11)	1020, 1019, 1018, 1046	0.818
'g' (12)	1141	0.22
'h' (13)	1064	0.22

4.5.1.1 Islanding Event (Scenario II)

In this event, the system was disconnected from the grid supply through a circuit breaker at a simulation time of t = 15 s. As the combined generation capacity of all the three DGs was less than the total load demands, the system frequency decreased. The total load before islanding was 5.89 MW, with DGs supplying a maximum of 5.50 MW at their rated conditions. The PICM of the proposed technique estimated a power imbalance of 0.39 MW in the system. The ILSM then captured and processed this power mismatch to determine the best combination of loads to be shed. The detailed load shedding parameters are shown in Table 4.10, and The frequency response for this event is shown in Figure 4.8. The stability index of load busses after the islanding event is presented in Table 4.11.

Table 4.10: Frequency stability parameters for islanding event (Scenario II).

Parameters	Prop	Adap-I	Adap-II	Conv
Power imbalance (MW)	0.39	0.39	0.39	0.39
Load shed amount (MW)	0.38	0.32	0.453	0.57
Excessive load shed (MW)	−0.001	−0.007	0.063	0.18
Loads switched off	2, 11	b, d (2,5)	7	1–5
Frequency undershoot (Hz)	49.453	49.452	49.48	49.1
Frequency overshoot (Hz)	-	-	50.28	50.5

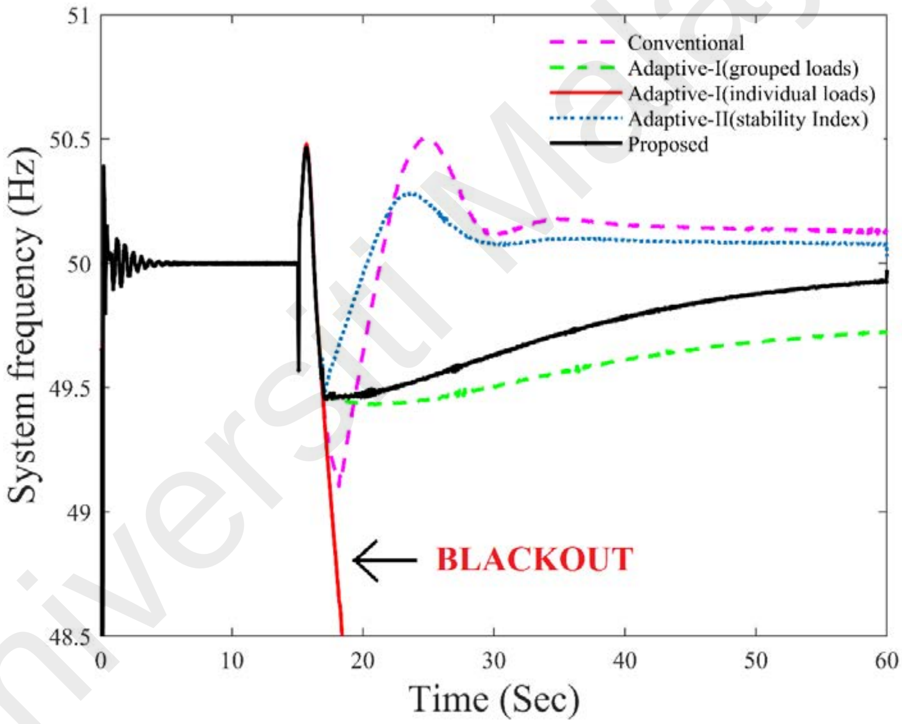

Figure 4.8: System frequency response (SFR) for islanding event (Scenario II).

It can be observed from Figure 4.8 and Table 4.10 that the conventional technique shed loads ranked 1–5 and resulted in a significant overshoot of 50.5 Hz and a lower undershoot in the system frequency. This was due to the extra number of loads being shed and the multistage load shedding, respectively. The results of the proposed method indicated a smoother frequency response without any overshoot and disconnected an optimal combination of the more unstable non-critical loads ranked 2 and 11, which exactly matched with an estimated power imbalance.

Table 4.11: Stability index of loads for the islanding event.

Sr. No	Proposed		Adaptive-I		Adaptive-II		Conventional	
	Rank	Stability	Rank	Stability	Rank	Stability	Rank	Stability
1	7	0.0757	7 (c)	0.0757	7	0.0757	7	0.0757
2	6	0.1686	6 (c)	0.1686	6	0.1686	6	0.1686
3	11	0.236	11 (f)	0.236	11	0.236	11	0.236
4	9	0.313	9 (f)	0.313	9	0.313	9	0.313
5	10	0.3161	10 (f)	0.3161	10	0.3161	10	0.3161
6	2	0.3267	2 (b)	0.3267	2	0.3267	2	0.3267
7	1	0.3336	1 (a)	0.3336	1	0.3336	1	0.3336
8	4	0.3448	4 (c)	0.3448	4	0.3448	4	0.3448
9	8	0.3491	8 (f)	0.3491	8	0.3491	8	0.3491
10	5	0.3619	5 (d)	0.3619	5	0.3619	5	0.3619
11	3	0.4244	3 (c)	0.4244	3	0.4244	3	0.4244
12	14	0.1975	14	0.1975	14	0.1975	14	0.1975
13	15	0.2487	15	0.2487	15	0.2487	15	0.2487
14	16	0.2644	16	0.2644	16	0.2644	16	0.2644
15	13	0.2964	13(h)	0.2964	13	0.2964	13	0.2964
16	12	0.4083	12 (g)	0.4083	12	0.4083	12	0.4083
17	18	0.0874	18	0.0874	18	0.0874	18	0.0874
18	17	0.2291	17	0.2291	17	0.2291	17	0.2291
19	20	0.2318	20	0.2318	20	0.2318	20	0.2318
20	19	0.2842	19	0.2842	19	0.2842	19	0.2842

Colored boxes show the load shed in the current event. proposed scheme, adaptive-I scheme, adaptive-II scheme, and conventional scheme

It can be seen from Table 4.10 and Table 4.11 that the load ranked 11 was disconnected instead of the more unstable loads 6 and 7 because disconnecting load 6 or load 7 would have caused an excessive load shedding, resulting in a high overshoot in the SFR, which can be seen for the SFR of the adaptive-II technique in Figure 4.8.

It was evident from Figure 4.8 that the Adaptive-I technique performed inadequate load shedding, as grouping of the loads limited the possible solutions. Any other solution for the Adaptive-I technique from Table 4.9 would have caused a very high overshoot. The stability of loads was also violated in the Adaptive-I technique as the second most stable load ranked 5 is disconnected (Table 4.11). Furthermore, the Adaptive-I technique based on an exhaustive search failed to perform load shedding at an appropriate time, when all the loads in the system were used for load shedding, which resulted in a cascaded blackout. This problem occurred because there are 1,048,575 possible combinations for 20 loads, and the computational time required to evaluate all these combinations was such that the system collapsed before the initialization of load shedding.

On the other hand, the Adaptive-II technique sheds first the most unstable load 7, as shown in Table 4.11. Table 4.10 shows that, although the Adaptive-II technique sheds the unstable load first, it shed an excessive 0.063 MW load in this event, causing an overshoot of 50.28 Hz due to excessive load shedding. However, the load shed amount for the proposed technique was optimal, as compared to the inadequate load shed amount of 0.32 MW and excessive load shed amounts of 0.453 MW and 0.57 MW for the Adaptive-II, and conventional techniques, respectively.

4.5.1.2 DG Tripping in an Islanded System (Scenario II)

For validation of the proposed method, one of the DGs was disconnected from the system during the islanded mode. The bio-mass DG was disconnected at time t = 60 s when the system was operating in islanded mode. Figure 4.9 shows the frequency response of the system, and frequency stability parameters are compared in Table 4.12. The conventional technique shed loads ranked 6–13 in addition to loads shed in Scenario 1, resulting in a frequency overshoot of 51.7 Hz. Loads ranked 'a' to 'g' in Table 4.9 were shed for the Adaptive-I technique. It is visible from Figure 4.9 that frequency was stabled for the proposed technique without any overshoot, as compared to an overshoot of 50.28 Hz, 53.6 HZ, and 51.7 Hz for the other techniques.

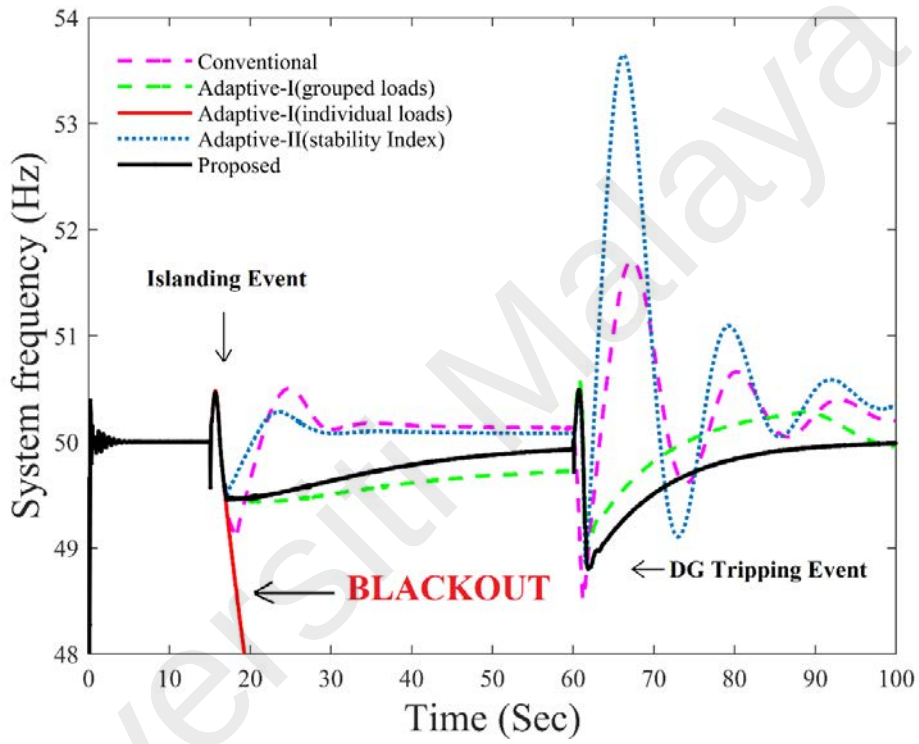

Figure 4.9: SFR for DG tripping event (Scenario II).

Table 4.12: Frequency stability parameters for DG tripping event (Scenario II).

Parameters	Prop	Adap-I	Adap-II	Conv
Power imbalance (MW)	1.891	1.891	1.891	1.89
Load shed amount (MW)	1.890	2.071	2.304	2.127
Excessive load shed (MW)	−0.001	0.18	0.414	0.237
Loads switched off	1, 4, 5, 6, 7, 10, 15	a, c, e–g (1,3,4,7-12)	1–6, 8-11, 14	6–13
Frequency undershoot (Hz)	48.8	49	48.86	48.54
Frequency overshoot (Hz)	-	50.28	53.6	51.7

Table 4.13: Stability index of load buses for DG-tripping event.

Sr. No	Proposed		Adaptive-I		Adaptive-II		Conventional	
	Rank	Stability	Rank	Stability	Rank	Stability	Rank	Stability
1	2	-	2 (b)	-	7	-	1	-
2	11	-	5 (d)	-	6	0.1667	2	-
3	7	0.0749	7 (e)	0.0749	11	0.2393	4	-
4	6	0.1667	6 (e)	0.1667	9	0.3186	5	-
5	9	0.3186	11(f)	0.2393	1	0.3206	3	-
6	1	0.3206	9 (f)	0.3186	10	0.3214	7	0.0749
7	10	0.3214	1 (a)	0.3206	2	0.3395	6	0.1667
8	4	0.3488	10 (f)	0.3214	4	0.3488	11	0.2393
9	8	0.3555	4 (c)	0.3488	8	0.3555	9	0.3186
10	5	0.3783	8 (f)	0.3555	5	0.3783	10	0.3214
11	3	0.4287	3 (c)	0.4287	3	0.4287	8	0.3555
12	14	0.1894	14	0.1894	14	0.1894	14	0.1894
13	15	0.2465	15	0.2465	15	0.2465	15	0.2465
14	16	0.2504	16	0.2504	16	0.2504	16	0.2504
15	13	0.2906	13 (h)	0.2906	13	0.2906	13	0.2906
16	12	0.4234	12 (g)	0.4234	12	0.4234	12	0.4234
17	18	0.0851	18	0.0851	18	0.0851	18	0.0851
18	20	0.2225	20	0.2225	20	0.2225	20	0.2225
19	17	0.2404	17	0.2404	17	0.2404	17	0.2404
20	19	0.285	19	0.285	19	0.285	19	0.285

Colored boxes show the load shed in the current event. proposed scheme, adaptive-I scheme, adaptive-II scheme, and conventional scheme.

The overshoot in the SFR for the Adaptive-I technique was due to the fact that the power imbalance was higher than the total random priority loads, and a fixed priority load was disconnected in addition to all random priority loads. Therefore, an additional 0.18 MW load was shed for the Adaptive-I technique, as can be seen in Table 4.12.

Table 4.13 indicates that the Adaptive-II technique sheds more unstable non-critical loads sequentially, to match with an estimated power imbalance. The power imbalance for this event was higher than the total non-critical loads. Therefore, the Adaptive-II technique sheds the most unstable load from the semi-critical loads, which was ranked 14. This resulted in an excessive load shed amount of 0.414 MW, causing a huge overshoot of 53.6 Hz in the SFR, whereas the proposed technique disconnected more unstable non-critical loads on priority and found an optimal combination of one semi-critical and six non-critical loads for this event. Table 4.13 shows that the proposed scheme selected unstable loads to match with the estimated power imbalance. It can be estimated from Table 4.12 that the load retained in the system was 5.72%, 11.5%, and 6.58% higher than the Adaptive-I, Adaptive-II, and conventional techniques, respectively. Therefore, the SFR in Figure 4.9 proves that the optimal amount of load was shed for the proposed technique, and the frequency response was smoother and more accurate than the conventional and adaptive techniques.

4.5.1.3 Overloading event in islanded system (Scenario II)

The practical load of an islanded system is usually variable. This variation in load causes instability in system frequency. The total load in the system may increase due to the additional load being connected to the system during islanded operation. This creates an imbalance between generation and load. Therefore, a practical load shedding scheme must be able to withstand this variation and stabilize the system frequency to avoid a blackout. To validate this condition, an additional load of 0.75 MW was intentionally connected in this scenario at time t = 60 s in the islanded system. All the four techniques discussed in this research were compared to this event. The stability index of loads for this scenario is shown in Table 4.14, the frequency response of the system is plotted inFigure 4.10, and Table 4.15 presents different parameters of load shedding.

Table 4.14: Stability index of load buses for the overloading event.

Sr. No	Proposed		Adaptive-I		Adaptive-II		Conventional	
	Rank	Stability	Rank	Stability	Rank	Stability	Rank	Stability
1	2	--	2 (b)	--	7	--	1	--
2	11	--	5 (d)	--	6	0.1689	2	--
3	7	0.0762	7 (e)	0.0762	11	0.2339	3	--
4	6	0.1689	6 (e)	0.1689	9	0.312	4	--
5	9	0.312	11 (f)	0.2339	10	0.3151	5	--
6	10	0.3151	9 (f)	0.312	2	0.3272	7	0.0762
7	1	0.3311	10 (f)	0.3151	1	0.3311	6	0.1689
8	4	0.3424	1 (a)	0.3311	4	0.3424	11	0.2339
9	8	0.3483	4 (c)	0.3424	8	0.3483	9	0.312
10	5	0.3631	8 (f)	0.3483	5	0.3631	10	0.3151
11	3	0.4216	3 (c)	0.4216	3	0.4216	8	0.3483
12	14	0.1941	14	0.1941	14	0.1941	14	0.1941
13	15	0.2437	15	0.2437	15	0.2437	15	0.2437
14	16	0.2615	16	0.2615	16	0.2615	16	0.2615
15	13	0.2959	13 (h)	0.2959	13	0.2959	13	0.2959
16	12	0.409	12 (g)	0.409	12	0.409	12	0.409
17	18	0.0875	18	0.0875	18	0.0875	18	0.0875
18	17	0.2295	17	0.2295	17	0.2295	17	0.2295
19	20	0.2301	20	0.2301	20	0.2301	20	0.2301
20	19	0.2804	19	0.2804	19	0.2804	19	0.2804

Colored boxes show the load shed in the current event. proposed scheme, adaptive-I scheme, adaptive-II scheme, and conventional scheme

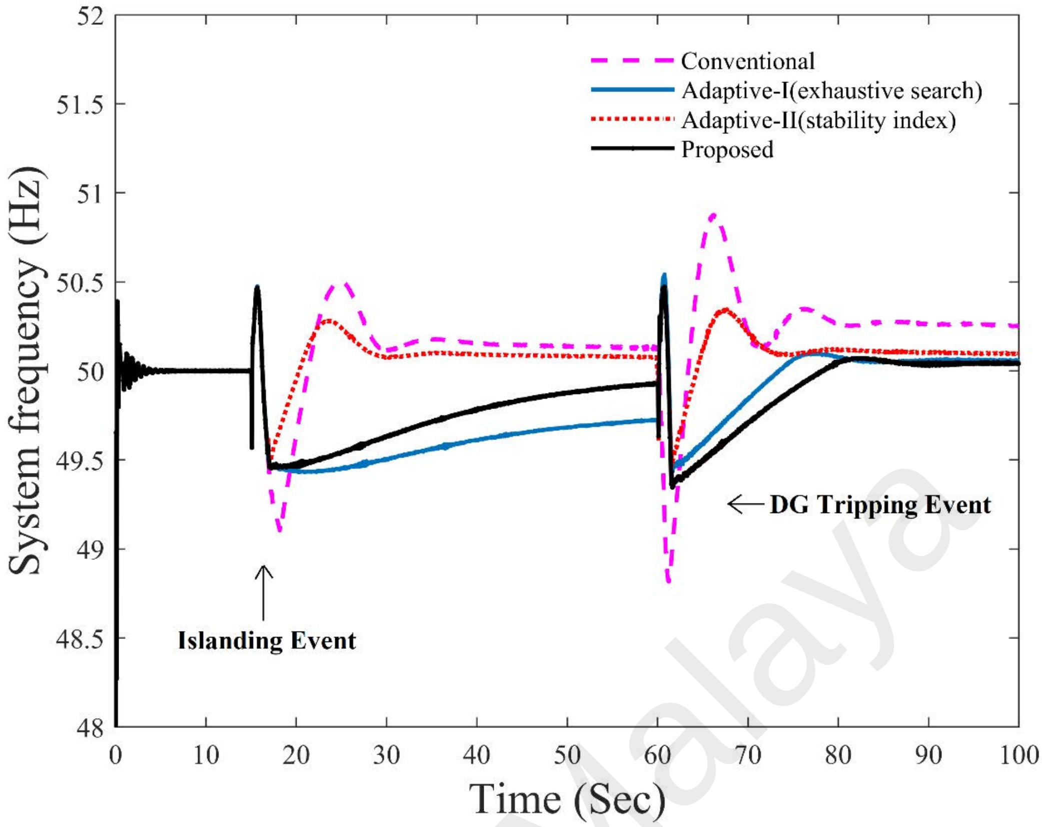

Figure 4.10: SFR for overloading event (Scenario II).

Table 4.15: Frequency stability parameters for overloading (Scenario II).

Parameters	Proposed	Adaptive-I	Adaptive-II	Conventional
Power imbalance (MW)	0.75	0.75	0.75	0.75
Excessive load shed (MW)	0.001	0.068	0.02	0.15
Loads switched off	7,8, 9	f (8-11)	6, 11	6, 7
Frequency undershoot (Hz)	49.38	49.43	49.44	48.81
Frequency overshoot (Hz)	50.07	50.09	50.33	50.87

It is visible from Table 4.15 that the conventional technique shed loads 6 and 7, in addition to loads 1 to 5 that were shed in the previous case, and caused a high overshoot of 50.87 Hz and excessive load shedding of 0.15 MW. The Adaptive-I technique also yielded an overshoot of 50.09 Hz, and the load ranked as ‘f’ in Table 4.9 was shed in addition to loads ‘b’ and ‘d’. It is evident from load priority table that the only possible solution for a power imbalance of 0.75 was to disconnect load ‘f’, which yielded excessive load shedding of 0.068 MW. The frequency response did not depict any prominent overshoot for the Adaptive-I technique because of the fact that inadequate load shedding was performed for the islanding event, as discussed in the islanding event. Conversely, the frequency was restored to the nominal value in the proposed technique by shedding the comparatively unstable loads ranked 7, 8, and 9 (Table 4.14) in addition to loads shed during the islanding event. The SFR for the Adaptive-II technique in Figure 4.10 indicates that excessive load shedding was performed due to sequential shedding of the most unstable loads ranked 6 and 11, as highlighted in Table 4.14, which yielded an overshoot of 50.33.

4.5.2 Test results for IEEE 69 bus system

In this case, islanding and DG-tripping events were simulated on the IEEE 69-bus system to validate the robustness of the proposed technique. Load shedding was performed using the proposed and both adaptive techniques discussed in the above sections.

4.5.2.1 Islanding Event (69-Bus System)

The grid-coupling circuit breaker was disconnected at a simulation time of t = 15 s to create intentional islanding for the IEEE 69-bus system. The total connected load in the system was 3.806 MW in this event, which was higher than the combined generation capacity of the DGs. Therefore, the PIFM estimated a power imbalance of 0.563 MW in the system, and the SICM calculated the stability index of all load buses. Loads were arranged in ascending order according to the stability index, incorporating load priority. Critical loads were not shed in any case; hence the stability indices of only non-critical and semi-critical loads are presented in Table 4.17. The system frequency response for this scenario is shown in Figure 4.11, and detailed load shedding parameters are presented in Table 4.16.

Table 4.16: Frequency stability parameters for Islanding (IEEE 69 bus system).

Parameters	Islanding Event		
	Proposed	Adaptive-II	Adaptive-I
Power imbalance (MW)	0.563	0.563	0.563
Excessive load shed (MW)	0	0.031	Blackout
Loads switched off	3, 4, 6, 7, 14, 16, 20	7,10,11, 12,13–24	
Frequency undershoot (Hz)	49.42	49.44	
Frequency overshoot (Hz)	-	50.09	

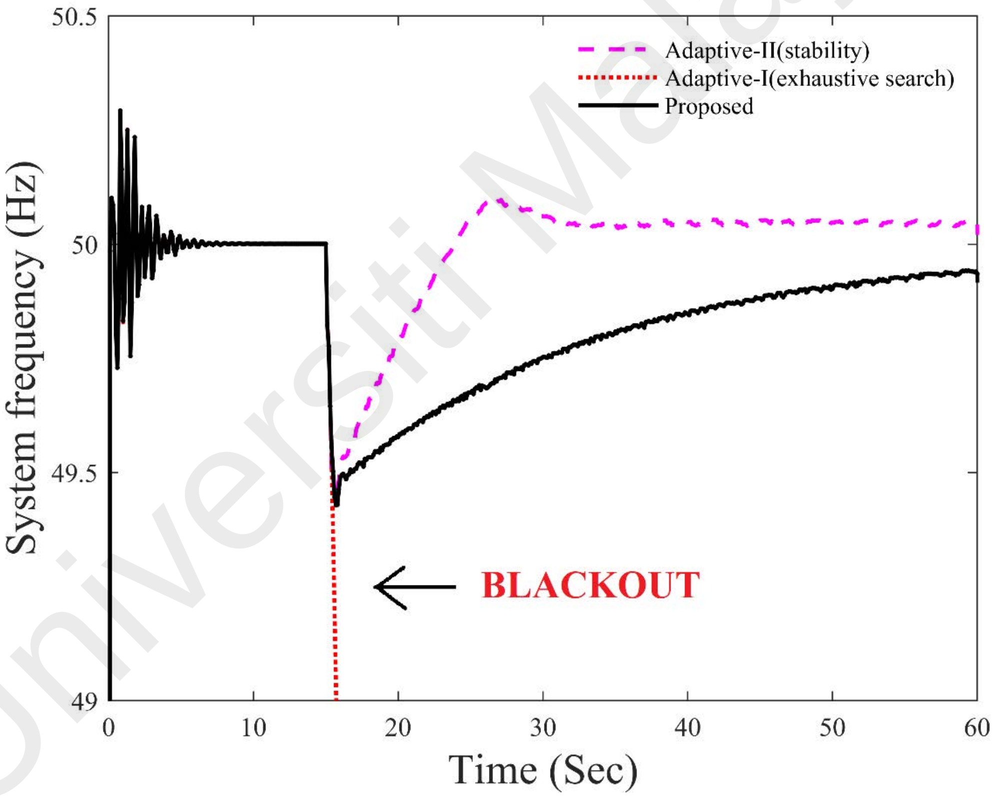

Figure 4.11: SFR comparison (IEEE 69-bus system).

The SFR in Figure 4.11 depicts that the adaptive technique based on an exhaustive search could not perform load shedding in time and result in a blackout. Possible combinations for 48 loads of the IEEE 69-bus system reached beyond 281 trillion. Therefore, it was infeasible for a practical computer system to store and evaluate all combinations, whereas the adaptive technique based on the stability index shed the unstable loads from Table 4.17 sequentially and resulted in an overshoot of 50.09 Hz (Figure 4.11). This overshoot in the SFR suggested that an additional load of 0.031 MW had been shed. On the other hand, the SFR for the proposed technique in Figure 4.11 indicated that an accurate amount of load was shed to avoid any overshoot. The stability index table and detailed load shedding parameters in Table 4.16 indicate that minimum and comparatively unstable non-critical loads were selected for shedding to ensure stable islanding operation of the distribution system.

Table 4.17: Stability index of loads for IEEE 69-bus System.

Sr. No	Islanding				DG Tripping			
	Proposed		Adaptive-II		Proposed		Adaptive-II	
	Rank	Stability	Rank	Stability	Rank	Stability	Rank	Stability
1	7	0.4995	7	0.4995	7	--	7	--
2	23	0.5135	23	0.5135	14	--	10	--
3	22	0.5179	22	0.5179	16	--	11	--
4	21	0.5344	21	0.5344	4	--	12	--
5	14	0.5399	14	0.5399	6	--	13	--
6	16	0.5987	16	0.5987	20	--	14	--
7	17	0.6075	17	0.6075	3	--	15	--
8	18	0.6108	18	0.6108	11	0.2039	16	--
9	11	0.6201	11	0.6201	23	0.2084	17	--
10	15	0.6276	15	0.6276	22	0.2089	18	--
11	13	0.6440	13	0.6440	21	0.2171	19	--
12	20	0.6483	20	0.6483	17	0.2233	20	--
13	12	0.6638	12	0.6638	18	0.2255	21	--
14	10	0.6731	10	0.6731	10	0.2298	22	--
15	24	0.6896	24	0.6896	15	0.2321	23	--
16	19	0.6896	19	0.6896	13	0.2332	24	--
17	4	0.7071	4	0.7071	12	0.2357	4	0.2343

Table 4.17 Continue

18	9	0.7128	9	0.7128	9	0.2403	9	0.2519
19	1	0.7290	1	0.7290	8	0.2449	8	0.252
20	8	0.7310	8	0.7310	5	0.2562	5	0.2587
21	2	0.7348	2	0.7348	2	0.2762	6	0.2672
22	3	0.7538	3	0.7538	1	0.2813	2	0.2765
23	5	0.7704	5	0.7704	24	0.2836	3	0.2766
24	6	0.7848	6	0.7848	19	0.2836	1	0.2837
25	31	0.5748	31	0.5748	31	0.2283	31	0.2379
26	30	0.5806	30	0.5806	30	0.2306	30	0.2404
27	29	0.5974	29	0.5974	29	0.2389	29	0.249
28	28	0.6144	28	0.6144	28	0.2469	28	0.2574
29	27	0.6254	27	0.6254	27	0.2522	27	0.2629
30	26	0.6399	26	0.6399	26	0.2591	36	0.2673
31	25	0.6746	25	0.6746	36	0.267	26	0.2702
32	36	0.7151	36	0.7151	35	0.276	35	0.2763
33	33	0.7303	33	0.7303	25	0.2767	25	0.2885
34	35	0.7344	35	0.7344	33	0.3233	33	0.331
35	32	0.7825	32	0.7825	32	0.3559	32	0.3641
36	34	0.7989	34	0.7989	34	0.365	34	0.3733

Colored boxes show the load shed in the current event. proposed scheme, adaptive-II scheme

4.5.2.2 DG-Tripping Event (IEEE 69-Bus System)

A DG was intentionally desynchronized from the islanded system to validate the performance of the proposed technique in case of a suspected cascaded blackout. One of the DGs in the system was disconnected at a simulation time of t = 60 s when the system was operating in stable islanding condition. The PICM estimated a power imbalance of 0.797 MW in the system for this event. Stability indices of connected loads for this event are arranged in ascending order and shown in Table 4.17. Stability indices of already disconnected loads in the islanding event are replaced by dashes in Table 4.17.

Table 4.18: Frequency stability parameters for DG tripping IEEE 69 bus system.

Parameters	DG Tripping Event		
	Proposed	Adaptive-II	Adaptive-I
Power imbalance (MW)	0.797	0.797	Blackout
Excessive load shed (MW)	0	0.125	
Loads switched off	2–7, 9–12, 14–17, 19–22, 24, 32, 33	1–31, 33, 35, 36	
Frequency undershoot (Hz)	49.39	49.53	
Frequency overshoot (Hz)	-	50.7	

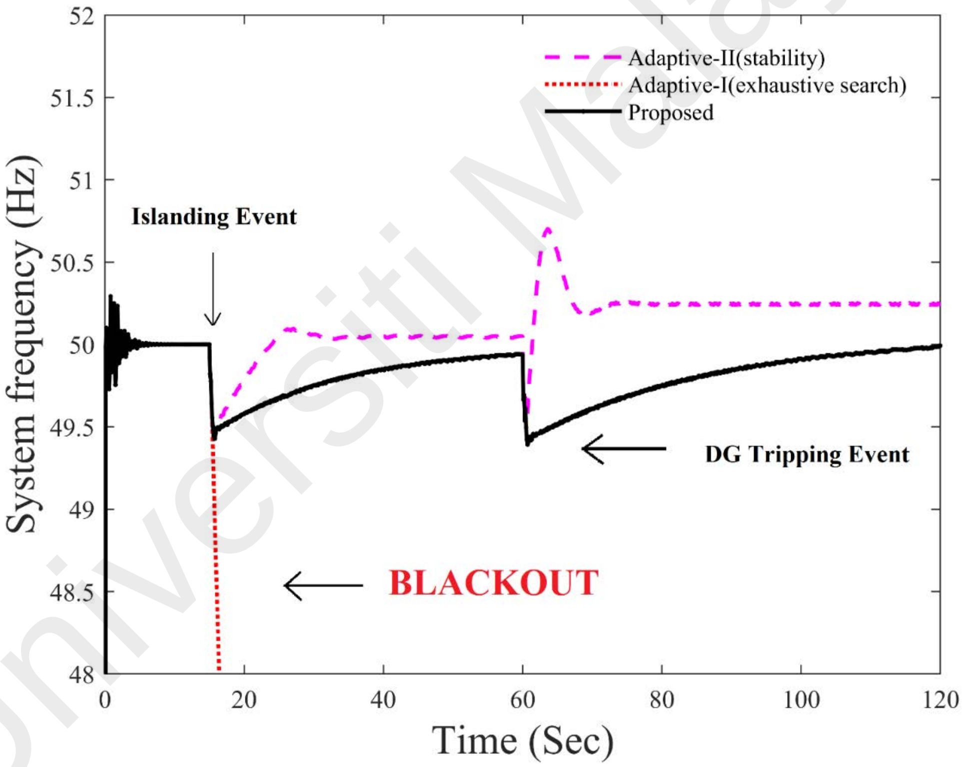

Figure 4.12: SFR comparison for DG tripping event (IEEE 69-bus system).

Table 4.17 indicates that all the non-critical and semi-critical loads except loads ranked 32 and 34 were disconnected for the adaptive-II technique based on the stability index, shedding an additional 0.125 MW load. The excessive load shedding caused a high overshoot of 50.7 in the SFR for the Adaptive-II technique. The SFR in Figure 4.12 and load shedding parameters in Table 4.18 shows that proposed techniques performed a better load shedding without any overshoot in the SFR by disconnecting a combination of two semi-critical and 19 non-critical loads in this event.

It is obvious to conclude from the simulation results in this scenario that the performance of the proposed technique was not affected by increasing the number of loads. However, the adaptive-I technique based on an exhaustive search failed to find the best combination of loads to be shed at an appropriate time, when all the loads in the system were used for load shedding, and this led the system frequency to drop in no time, which resulted in a cascaded blackout. On the other hand, adaptive-II technique increases voltage stability; however, sequential selection of unstable loads yields very high overshoots in frequency response. This high overshoots beyond the frequency threshold of 50.5 Hz cause serious stability problems for an islanded system. The proposed technique resulted in smoother frequency response by disconnecting more unstable and non-critical loads on priority. Furthermore, the connected load after the islanding and DG-tripping events was maximum for the proposed technique.

4.6 Scenario III

The main objective of all the load shedding techniques was to maximize load connection in the system with a stable frequency. It is visible from the comparison of results in the above scenarios that a maximum load was connected in the system for the proposed technique. Moreover, the proposed load shedding scheme selected an optimal combination of loads for any contingency, incorporating load priority and the stability index to produce an SFR without any significant overshoot. The advantage of incorporating load priority and the stability index simultaneously for a load shedding technique is analyzed in this scenario. The proposed technique was simulated with three different objective functions, as shown in Equations (4.3) to (4.5), for load shedding. The basic objective function for the proposed mathematical model found an optimal combination of loads that exactly matched an estimated power imbalance, shown in Equation (4.3).

$$OF_1 = \min\left[\sum_{i=1}^{N} A_i.x_i + \delta.w\right] \tag{4.3}$$

$$OF_2 = \min\left[\sum_{i=1}^{N} SI_i.x_i + \delta.w\right] \tag{4.4}$$

$$OF_3 = \min\left[\sum_{j\in NCL} \alpha.SI_j.x_j + \sum_{k\in SCL} \beta.SI_k.x_k + \sum_{l\in CL} \gamma.SI_l.x_l + \delta.w\right] \tag{4.5}$$

Where *A* denotes the uniform priority of loads, *α, β* and *γ* are proposed priority of loads, *x* is the binary variable that shows the status of circuit breaker; 0 for disconnected and 1 for connected, *SI* is the stability index of load busses, *w* is the dummy variable for MILP optimization to satisfy the constraints and δ is its coefficient. The objective function in Equation (4.3) will estimate a combination of loads from all the system loads without any load priority. This function can be modified to include the stability index of loads for load shedding, as shown in Equation (4.4). Including the stability index improves the voltage profile of the system as the buses with more unstable voltages are preferred for load shedding. The reliability of the system can be improved by assuring the supply to critical and semi-critical loads. Therefore, the objective function proposed for this technique shown in Equation (4.5) utilizes the load priority based on voltage stability index and type of load simultaneously to disconnect more unstable and non-critical loads first. Semi-critical loads are only shed when the power imbalance is more than the total non-critical load in the system. Intentional islanding and DG-tripping events are simulated.

4.6.1 Islanding Event (Scenario III)

The grid-coupling circuit breaker was operated at a simulation time of *t* = 15 s to implement intentional islanding. The generation capacity of all DGs in the system was less than the total load demand, and frequency started decreasing. The proposed PIFM estimated a power imbalance of 0.39 MW in this case and activated the SICM and ILSM. The SICM then processed the system data to calculate the stability indices of all load buses and transmitted them to the ILSM. The load shedding module found the optimal combination of loads to be shed as directed by the objective functions. Stability indices of all loads are summarized in Table 4.11.

It is evident from Figure 4.13 that the SFR was similar in the islanding event for all three proposed objective functions. This was due to the fact that the power imbalance was smaller, and the mathematical model found a unique solution that fulfilled constraints for all three objective functions. Hence optimal load shedding was performed. Table 4.19 also shows that loads ranked 2 and 11 were selected for shedding with minimum error and no overshoot.

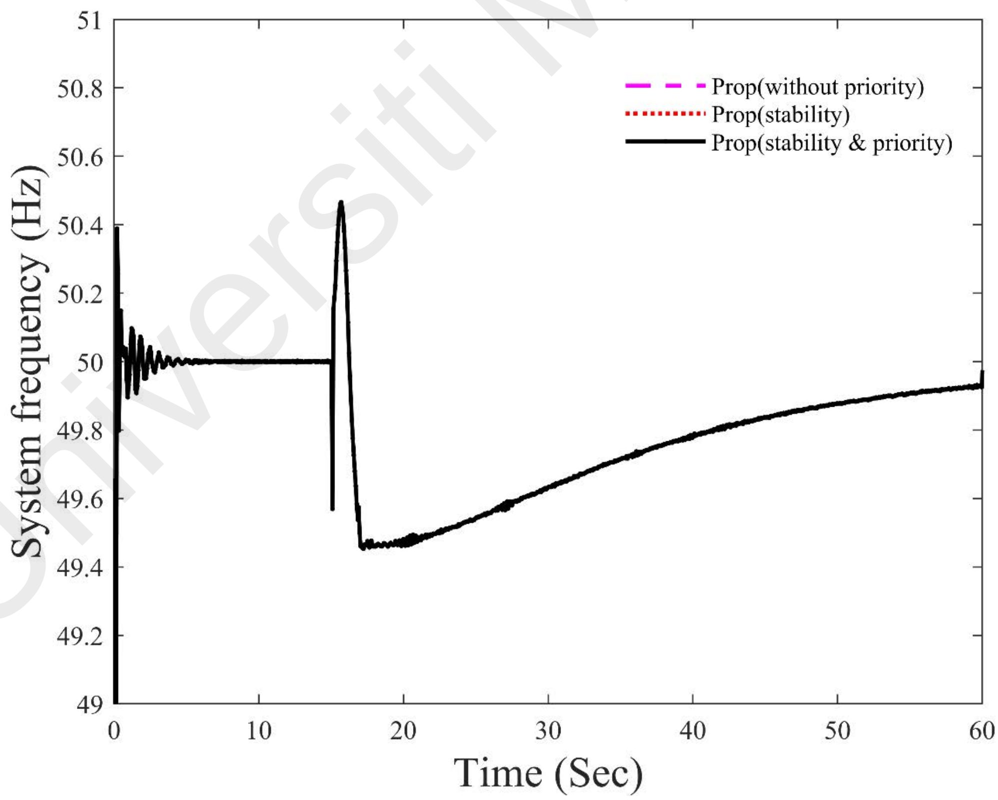

Figure 4.13: SFR comparison for the proposed technique (Islanding).

Table 4.19: Load shedding parameters for the proposed scheme (islanding).

Parameters	Prop.St.Pr	Pro.St	Prop(W/O) Priority
Power imbalance (MW)	0.39	0.39	0.39
Additional load disconnected (MW)	0.001	0.001	0.001
Loads switched off	2, 11	2, 11	2, 11
Frequency undershoot (Hz)	49.453	49.453	49.453
Frequency overshoot (Hz)	-	-	-

4.6.2 DG Tripping in Islanded System (Scenario III)

The biggest DG in the system was disconnected at a simulation time of t = 60 s to validate the proposed technique. The system frequency declined rapidly, and the PICM actuated load shedding, and it forecasted a power imbalance of 1.891 MW.

Table 4.20: Load shedding parameters for the proposed scheme (DG tripping).

Parameters	Prop.St.Pr	Prop.St	Prop(W/O) Priority
Power imbalance (MW)	1.891	1.891	1.891
Additional load disconnected (MW)	−0.001	0	0
Loads switched off	1, 4, 5, 6, 7, 10, 15	7, 8, 10, 14, 15, 16	1, 4, 6, 7, 8, 14, 16
Frequency undershoot (Hz)	48.8	48.89	48.78
Frequency overshoot (Hz)	-	50.03	50.01

The SFR in Figure 4.14 for the DG-tripping event reveals that accurate load shedding was performed for the proposed technique with all three objective functions. An almost similar amount of load was shed with the three different solutions for all discussed objective functions. The stability index of all loads for this contingency is shown in Table 4.13.

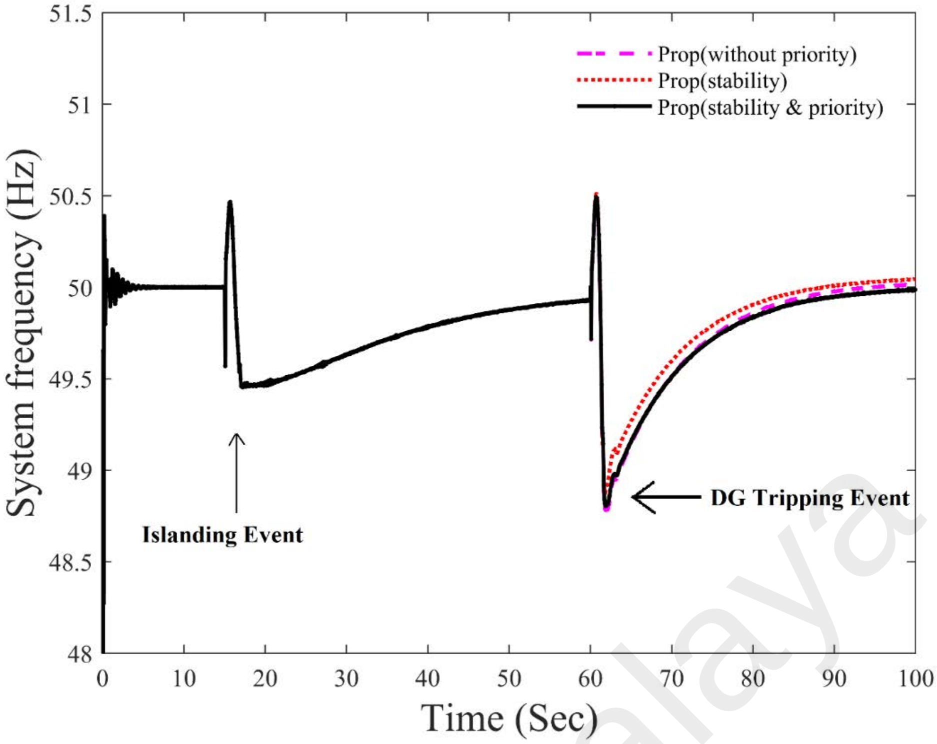

Figure 4.14: SFR comparison for the proposed technique (DG tripping).

It can be observed from Table 4.13 and Table 4.20 that semi-critical loads 14, 15, and 16 were switched off when the proposed technique was tested with the load priority based on the stability index only. On the other hand, comparatively stable and semi-critical loads 14 and 16 were shed when the proposed technique was tested without any load priority. Therefore, it is conclusive that the proposed technique performed better and disconnected more unstable and non-critical loads when loads were prioritized based on both their type and stability index simultaneously. Semi-critical and stable loads were disconnected from the system when it was simulated without any load priority and stability. Furthermore, it can be observed from Figure 4.13, Figure 4.14, Table 4.19, and Table 4.20 that a load shedding solution that incorporated the stability index and load priority simultaneously increased the reliability of the power supply for critical loads and improved the stability of load buses. Hence, the proposed load shedding scheme based on polynomial regression, MILP optimization, stability index, and load priority solved the load shedding problem much more efficiently, and its performance was not affected, regardless of the number of loads.

4.7 Summary

This chapter presented the validation of the proposed technique for under frequency load shedding. All the simulation results obtained from PSCAD/EMTDC depict that the proposed technique successfully performed optimal load shedding for all scenarios. It was validated that the frequency reaches in the normal operating region (49.5-50.5) of turbine within appropriate time. The settling time of frequency response for proposed scheme may be a bit high. However, optimal and accurate amount of load disconnection results in a slow and smooth recovery of frequency response ensuring safe turbine operation. Furthermore, it is evident form the results that increasing number of loads for a large-scale system does not affect the performance of the proposed technique. Whereas the adaptive technique presented in literature based on exhaustive search could not converge when the number of loads increases beyond a limit and results in system blackout. Moreover, power imbalance estimation incorporating the proposed algorithm handles the non-linearities in the system for extreme and varying loading conditions.

CHAPTER 5: CONCLUSION AND FUTURE WORKS

5.1 Conclusion

A modern grid integrates a large number of DGs based on renewable energy. The intermittency of DGs often creates a power imbalance in the distribution system, leading to cascaded blackout when the system is disconnected from the grid. An effective way to counter the grid-failure is by deploying an efficient load shedding scheme. A simple sequential or random load shedding may balance the grid power, but it affects the system frequency leading to overall grid instability. The absence of load priority endangers the functionality of vital loads. Moreover, disconnecting load busses with stable voltage may result in operation of under-voltage protection. Therefore, it is crucial to find the optimal load shedding mechanism.

Formulating a new power imbalance equation is crucial for a load shedding scheme to increase the accuracy. A new power imbalance equation is proposed based on a simple polynomial regression method. The rate of change of frequency is used to estimate power imbalance, and MILP optimization is used to find the optimal combination from the prioritized loads. The proposed scheme is validated on three different test systems (a 28-bus system part of the Malaysian distribution network, the IEEE 69-bus system, and the IEEE 137 bus system) by simulating different events such as islanding, generator tripping, and overloading Simulation results show that the proposed technique finds a more accurate power imbalance, especially in extreme conditions, i.e., cascaded DG outage.

An exhaustive search scheme is an inefficient way to load shedding as it can only work for a limited number of loads. Increasing the number of loads yields a huge number of possible combinations and thus requires a large memory size to sort these combinations (281 trillion for 69-bus system loads and 7.92*1028 for IEEE 137 bus system). Moreover, it is infeasible to evaluate all the possible combinations that will require high computational time. A blackout occurs for the large-scale systems due to the delayed response and infeasible computation memory requirement for an exhaustive search. This thesis proposed an optimal load shedding scheme using MILP optimization to achieve the power balance. The salient features of the proposed scheme are: (1) it is not dependent on the number of loads connected to the grid (2) Less computational time (3) A smooth frequency response with optimal load shedding.

Voltage stability can be enhanced by shedding more unstable loads on priority to avoid unnecessary operation of under-voltage protection. The conventional method of sequential shedding of unstable loads yields excessive load shedding, resulting in overshoot, and endangers the stability of system frequency. On the other hand, prioritized shedding of comparatively more unstable non-critical loads produces a smooth recovery of frequency response without any overshoot. The proposed algorithm increases the system voltage stability by disconnecting more unstable loads on priority, thus preventing the triggering of under-voltage protection.

Integrating proposed power imbalance estimation with disconnecting optimal combination of loads based on stability index and load priority results in an efficient under frequency load shedding technique. Simulation results prove that the proposed technique is an optimal solution to the load shedding problem for a distribution network.

5.2 Future works

The high share of non-synchronous generation sources in future power systems presents low or no inertia. As a result, power imbalance estimation for load shedding based on the rate of change of frequency and inertia of the system may not be reliable and efficient in practice. Moreover, AC/DC microgrids are gaining traction in modern power systems. Therefore, future work on this technique will be to propose a new load shedding scheme to mitigate the effect of low inertia of the system. Furthermore, the bidirectional power share in modern AC/DC microgrids will be investigated to avoid load shedding and maximize the power supply in the system. These future works are summarized as follows:

1. Propose a new power imbalance estimation independent of system frequency for low inertia microgrids.
2. Analyze the impact of low inertia on the swing equation for a modern power system.
3. Investigate AC/DC microgrids for bidirectional power flow to avoid load shedding for small contingencies.
4. Design a composite AC and DC load shedding to stabilize the system voltage and frequency under all circumstances.

REFERENCES

Anderson, P. M., & Mirheydar, M. (1992). An adaptive method for setting underfrequency load shedding relays. *Ieee Transactions on Power Systems, 7*(2), 647-655.

Azmy, A. M., & Erlich, I. (2005, 16-16 June 2005). *Impact of distributed generation on the stability of electrical power system.* Paper presented at the IEEE Power Engineering Society General Meeting, 2005.

Barker, P. P., & Mello, R. W. D. (2000, 16-20 July 2000). *Determining the impact of distributed generation on power systems. I. Radial distribution systems.* Paper presented at the 2000 Power Engineering Society Summer Meeting (Cat. No.00CH37134).

Caliskan, S. Y., & Tabuada, P. (2015, 15-18 Dec. 2015). *Uses and abuses of the swing equation model.* Paper presented at the 2015 54th IEEE Conference on Decision and Control (CDC).

Chakravorty, M., & Das, D. (2001). Voltage stability analysis of radial distribution networks. *International Journal of Electrical Power & Energy Systems, 23*(2), 129-135.

Çimen, H., & Aydın, M. (2015). Optimal Load Shedding Strategy for Selçuk University Power System with Distributed Generation. *Procedia-Social and Behavioral Sciences, 195*, 2376-2381.

Davis, M. W. (2002a, 21-25 July 2002). *Distributed resource electric power systems offer significant advantages over central station generation and T & D power systems. II.* Paper presented at the IEEE Power Engineering Society Summer Meeting.

Davis, M. W. (2002b, 21-25 July 2002). *Distributed resource electric power systems offer significant advantages over central station generation and T&D power systems. I.* Paper presented at the IEEE Power Engineering Society Summer Meeting.

Dreidy, M., Mokhlis, H., & Mekhilef, S. J. E. (2017). Application of meta-heuristic techniques for optimal load shedding in islanded distribution network with high penetration of solar PV generation. *10*(2), 150.

Ford, J. J., Bevrani, H., & Ledwich, G. (2009). Adaptive load shedding and regional protection. *International Journal of Electrical Power & Energy Systems, 31*(10), 611-618.

Gautam, M., Bhusal, N., & Benidris, M. (2020, 6-7 Feb. 2020). *A Sensitivity-based Approach to Adaptive Under-Frequency Load Shedding.* Paper presented at the 2020 IEEE Texas Power and Energy Conference (TPEC).

Girgis, A. A., & Ham, F. M. (1982). A New FFT-Based Digital Frequency Relay for Load Shedding. *IEEE Transactions on Power Apparatus and Systems, PAS-101*(2), 433-439.

Haes Alhelou, H., Hamedani-Golshan, M. E., Njenda, T. C., & Siano, P. (2019). Wide-area measurement system-based optimal multi-stage under-frequency load-shedding in interconnected smart power systems using evolutionary computing techniques. *Applied Sciences, 9*(3), 508.

Hooshmand, R., & Moazzami, M. (2012). Optimal design of adaptive under frequency load shedding using artificial neural networks in isolated power system. *International Journal of Electrical Power & Energy Systems, 42*(1), 220-228.

IEEE.Standard.242. (2001). IEEE Recommended Practice for Protection and Coordination of Industrial and Commercial Power Systems (IEEE Buff Book). *IEEE Std 242-2001 (Revision of IEEE Std 242-1986) [IEEE Buff Book]*, 1-710.

IEEE.Standard.1547. (2003). *IEEE Standard for Interconnecting Distributed Resources with Electric Power Systems: 1547-2003*: IEEE.

IEEE.Standard.94248. (2003). IEEE Guide for Protective Relaying of Utility-Consumer Interconnections. *IEEE Std C37.95-2002 (Revision of IEEE Std C37.95-1989)*, 1-58.

Jiang, H., Yan, G., Ji, H., Liu, L., & Shan, D. (2010). *An improved under frequency load shedding scheme based on rate of change of frequency.* Paper presented at the International Conference on Electrical and Control Engineering (ICECE), 2010.

Karimi, M., Mohamad, H., Mokhlis, H., & Bakar, A. (2012). Under-frequency load shedding scheme for islanded distribution network connected with mini hydro. *International Journal of Electrical Power & Energy Systems, 42*(1), 127-138.

Karimi, M., Wall, P., Mokhlis, H., & Terzija, V. (2017). A new centralized adaptive underfrequency load shedding controller for microgrids based on a distribution state estimator. *Ieee Transactions on Power Delivery, 32*(1), 370-380.

Khezri, R., Golshannavaz, S., Vakili, R., & Memar-Esfahani, B. (2017). Multi-layer fuzzy-based under-frequency load shedding in back-pressure smart industrial microgrids. *Energy, 132*, 96-105.

Laghari, J. A., Mokhlis, H., Bakar, A. H. A., & Mohamad, H. (2013). Application of computational intelligence techniques for load shedding in power systems: A review. *Energy Conversion and Management, 75*, 130-140.

Laghari, J. A., Mokhlis, H., Karimi, M., Abu Bakar, A. H., & Mohamad, H. (2015). A New Under-Frequency Load Shedding Technique Based on Combination of Fixed and Random Priority of Loads for Smart Grid Applications. *Ieee Transactions on Power Systems, 30*(5), 2507-2515.

Li, Y., & Zhang, B. (2014). *A new adaptive load shedding control strategy based on the transient voltage disturbance scale detection in power systems.* Paper presented at the 14th International Conference on Environment and Electrical Engineering (EEEIC), 2014

Lopes, J. A. P., Moreira, C. L., & Madureira, A. G. (2006). Defining control strategies for MicroGrids islanded operation. *Ieee Transactions on Power Systems, 21*(2), 916-924.

López, K., Pérez, S., & Rodríguez, L. (2016). Optimal under voltage load shedding based on voltage stability index. *Ingeniería e Investigación, 36*(2), 43-50.

Meegahapola, L., & Flynn, D. (2010, 25-29 July 2010). *Impact on transient and frequency stability for a power system at very high wind penetration.* Paper presented at the IEEE PES General Meeting.

Moazzami, M., Khodabakhshian, A., & Hooshmand, R.-A. (2015). A New Optimal Under-frequency Load-shedding Method Using Hybrid Culture–Particle Swarm Optimization–Co-evolutionary Algorithm and Artificial Neural Networks. *Electric Power Components and Systems, 43*(1), 69-82.

Mohammadi-Ivatloo, B., Mokari, A., Seyedi, H., Ghasemzadeh, S. J. J. o. O., & Engineering, A. i. P. (2014). An improved under-frequency load shedding scheme in distribution networks with distributed generation. *2*(1), 22-31.

Mokari-Bolhasan, A., Seyedi, H., Mohammadi-ivatloo, B., Abapour, S., & Ghasemzadeh, S. (2014). Modified centralized ROCOF based load shedding scheme in an islanded distribution network. *International Journal of Electrical Power & Energy Systems, 62*, 806-815.

Muhammad, M. A., Mokhlis, H., Naidu, K., Amin, A., Franco, J. F., & Othman, M. (2019). Distribution Network Planning Enhancement via Network Reconfiguration and DG Integration using Dataset Approach and Water Cycle Algorithm. *Journal of Modern Power Systems and Clean Energy*, 1-8.

Narula, K., Nagai, Y., & Pachauri, S. (2012). The role of Decentralized Distributed Generation in achieving universal rural electrification in South Asia by 2030. *Energy Policy, 47*, 345-357.

Nourollah, S., Aminifar, F., & Gharehpetian, G. B. (2018). A Hierarchical Regionalization-Based Load Shedding Plan to Recover Frequency and Voltage in Microgrid. *Ieee Transactions on Smart Grid*.

Pan, T., Xu, D., Li, Z., Shieh, S.-S., & Jang, S.-S. (2013). Efficiency improvement of cogeneration system using statistical model. *Energy Conversion & Management, 68*, 169-176.

Potel, B., Debusschere, V., Cadoux, F., & Rudez, U. (2019). A Real-Time Adjustment Method of Conventional Under-Frequency Load Shedding Thresholds. *Ieee Transactions on Power Delivery*.

Qing, H., Shicong, M., Jun, Y., & Guangquan, B. (2016). *Research on the application of intelligent under-frequency/under-voltage load shedding considering demand response.* Paper presented at the China International Conference on Electricity Distribution (CICED), 2016.

Rafinia, A., Moshtagh, J., & Rezaei, N. (2020). Stochastic optimal robust design of a new multi-stage under-frequency load shedding system considering renewable energy sources. *International Journal of Electrical Power & Energy Systems, 118*, 105735.

Reddy, C., Chakrabarti, S., & Srivastava, S. (2014). A sensitivity-based method for under-frequency load-shedding. *Ieee Transactions on Power Systems, 29*(2), 984-985.

Rudez, U., & Mihalic, R. (2011). A novel approach to underfrequency load shedding. *Electric Power Systems Research, 81*(2), 636-643.

Santamouris, M., Cartalis, C., Synnefa, A., & Kolokotsa, D. (2015). On the impact of urban heat island and global warming on the power demand and electricity consumption of buildings—A review. *Energy & Buildings, 98*, 119-124.

Santos, A. Q., Monaro, R., Coury, D., & Oleskovicz, M. (2014). Real-time closed loop system controlled by an Artificial Neural Network for estimation of the optimal load shedding.

Santos, A. Q., Monaro, R. M., Coury, D. V., & Oleskovicz, M. (2019). A new real-time multi-agent system for under frequency load shedding in a smart grid context. *Electric Power Systems Research, 174*, 105851.

Santos, A. Q., Shaker, H. R., & Jørgensen, B. N. (2018, 21-23 Nov. 2018). *A Holistic Fuzzy Measure for Load Priority in Under Frequency Load Shedding Schemes.* Paper presented at the 2018 International Symposium on Advanced Electrical and Communication Technologies (ISAECT).

Savier, J. S., & Das, D. (2007). Impact of Network Reconfiguration on Loss Allocation of Radial Distribution Systems. *IEEE Transactions on Power Delivery, 22*(4), 2473-2480.

Silva, M., Morais, H., & Vale, Z. (2012). An integrated approach for distributed energy resource short-term scheduling in smart grids considering realistic power system simulation. *Energy Conversion & Management, 64*, 273-288.

Taylor, C. W. (1992). Concepts of undervoltage load shedding for voltage stability. *Ieee Transactions on Power Delivery, 7*(2), 480-488.

Wang, Z., Guo, L., Wu, K., Liu, W., & Zhou, J. (2014). *Minimum load-shedding calculation approach considering loads difference.* Paper presented at the IEEE Innovative Smart Grid Technologies-Asia (ISGT Asia), 2014

Williams, J. H., DeBenedictis, A., Ghanadan, R., Mahone, A., Moore, J., Morrow Iii, W. R., . . . Torn, M. S. (2012). The Technology Path to Deep Greenhouse Gas Emissions Cuts by 2050: The Pivotal Role of Electricity. *Science, 335*(6064), 53-59.

Yan, J., Li, C., & Liu, Y. (2017). *Adaptive load shedding method based on power imbalance estimated by ANN.* Paper presented at the IEEE Region 10 Conference, TENCON 2017-2017.

Ye, L., Baohui, Z., Zhiqian, B., & Junzhe, L. (2015). *An adaptive load shedding method based on the underfrequency and undervoltage combined relay.* Paper presented at the 34th Chinese Control Conference (CCC), 2015

Yusof, N. A., Mohd Rosli, H., Mokhlis, H., Karimi, M., Selvaraj, J., & Sapari, N. M. (2017). A new under-voltage load shedding scheme for islanded distribution system based on voltage stability indices. *12*(5), 665-675.

Zhou, J., & Ohsawa, Y. (2009). Improved Swing Equation and Its Properties in Synchronous Generators. *IEEE Transactions on Circuits and Systems I: Regular Papers, 56*(1), 200-209.

Zhou, Q., Li, Z., Wu, Q., & Shahidehpour, M. J. I. T. o. S. G. (2018). Two-Stage Load Shedding for Secondary Control in Hierarchical Operation of Islanded Microgrids.

LIST OF PUBLICATIONS

1. **Sarwar, S.;** Mokhlis, H.; Othman, M.; Muhammad, M.A.; Laghari, J.A.; Mansor, N.N.; Mohamad, H.; Pourdaryaei, A. A Mixed Integer Linear Programming Based Load Shedding Technique for Improving the Sustainability of Islanded Distribution Systems. *Sustainability* **2020**, *12*, 6234.
2. **Sohail Sarwar[1],** Hazlie Mokhlis[1*], Mohamadariff Othman[1], Munir Azam Muhammad[1]. *"A new frequency stabilization technique for islanded distribution network based on polynomial regression and mixed integer linear programming."* Journal of modern power systems and clean energy. 2020

(Submitted, Under review)